THE LEFT VENTRICULAR PRESSURE-THICKENING LOOP: A POTENTIAL APPROACH TO THE ASSESSMENT OF TRANSMURAL MYOCARDIAL WORK

Mitchell Todd Saltzberg

Yale University

1992

The Left Ventricular Pressure-Thickening Loop: A Potential Approach to the Assessment of Transmural Myocardial Work

A Thesis Submitted to the Yale University School of Medicine in Partial Fulfillment of the Requirements for the Degree of Doctor of Medicine

by

Mitchell Todd Saltzberg

May 1992

THE PRESSURE - THICKENING LOOP: A POTENTIAL APPROACH TO THE ASSESSMENT OF TRANSMURAL MYOCARDIAL WORK. Mitchell Todd Saltzberg, Lawrence Young, Qing Xin Shi, Albert J. Sinusas (Yale University School of Medicine; Section of Cardiovascular Medicine, Department of Medicine, New Haven, CT)

Regional myocardial work can be determined from analysis of pressure-length loops derived using implanted paired ultrasonic crystals. A recently developed epicardial Doppler thickening crystal (DTC) technique offers an atraumatic means of assessing myocardial thickening at the sub-transmural (endocardial (EN), midwall (MW) and epicardial (EP)) level. We employed the DTC technique in 5 open chest dogs subjected to graded dobutamine (DB)(2.5 to 15 ug/kg/min) stress, to determine if the area of transmural (TM) and sub-transmural pressure-thickening loops (PTL) provided an index of regional work. Sub-transmural PTL were generated in the left anterior descending (LAD) perfusion territory and correlated with sub-transmural LAD microsphere flow, cardiac output (CO), hemodynamic indices of myocardial work (rate-pressure product (RPP) and maximal dP/dt (dP/dt)), and regional oxygen consumption (MVO_2). MVO_2 was determined from analysis of paired arterial and great cardiac vein blood samples. DB (10 ug/kg/min) caused an increase in; TM flow (baseline(B): 0.97+/-0.14 ml/min/gm; DB: 2.08+/-0.47 ml/min/gm), TM % thickening fraction (%TF) (B: 16.71+/-3.4 %; DB: 27.7+/-1.8%), CO (B: 2.5+/-0.3 l/min; DB: 4.5+/-0.6 l/min), RPP (B: 14941+/-2151; DB: 25377+/-1032), dP/dt (B: 1800+/-329; DB: 4614+/-731) and MVO_2 (B: 10.7+/-2.4 ml O_2/min/100 gm; DB: 13.3+/-0.8 ml O_2/min/100 gm). The serial changes in the area of the LAD TM PTL correlated with the changes in TM flow ($r=0.63$, $p<.05$), RPP ($r=0.65$, $p<.01$), dP/dt ($r=0.81$, $p<.01$), and regional MVO_2 ($r=0.52$, $p<.05$). Changes in LAD TM flow also significantly correlated with changes in RPP ($r=0.91$, $p<.01$), dP/dt ($r=0.86$, $p<.01$) and regional MVO_2 ($r=0.89$, $p<.01$), supporting the use of sub-transmural flow as an indirect index of sub-transmural work. The changes in LAD sub-transmural PTL area significantly correlated with flow changes in the MW ($r=0.57$, $p<.05$) and EP ($r=0.68$, $p<.01$) but not EN ($r=0.26$, p=NS) sub-regions.

Thus, regional PTL area correlated with regional flow and accepted indices of both regional and global work. The correlation of sub-transmural PTL area with sub-transmural flow suggests that PTL analysis holds promise as a potential index of changes in sub-transmural myocardial work.

Table of Contents

Introduction

Several approaches to the assessment of regional myocardial function have been taken both clinically and experimentally. A recently developed Doppler based technique to measure contractile function is thought to be a more reliable, reproducible and physiologic method to assess regional function. This approach provides a unique layer by layer assessment of transmural thickening. The purpose of this thesis is to evaluate the potential role of a novel methodology for the assessment of regional cardiac work at multiple levels by examining the relationship between transmural thickening and left ventricular pressure. We have preliminarily tested this approach to cardiac work in normal animals under conditions of increased demand. In this paper, the background which provides the framework from which this method of analysis was developed as well as potential applications on the clinical level will be outlined with an emphasis on the methodologies undertaken.

Clinical Perspective

Accurate clinical risk stratification based on myocardial viability and function is critical to the proper management of patients with coronary artery disease. This is especially true in the post myocardial infarction patient where the need to assess viability is paramount. While infarcted myocardium is known to be rendered nonfunctional, the consequences of an ischemic insult to the myocardium insufficient to cause necrosis may still result in a deterioration in function which may persist for an extended period of time after the initial insult. This functional deterioration associated with transient ischemia has been described by several authors as myocardial "stunning" [1-4]. Inherent to this concept of "stunning" is a dissociation in the relationship between myocardial flow and function. Braunwald first summarized this concept in 1982 where he described "stunning" as a situation in which:

> "An ischemic insult not of sufficient severity or duration to produce myocardial necrosis may acutely affect myocardial repolarization and cause angina (hit); but these changes wane rapidly (run), when the balance between myocardial oxygen supply and demand has been reestablished. However, the ischemia may interfere with normal myocardial function, biochemical processes and ultrastructure for prolonged periods (stun).[1]"

The duration of myocardial dysfunction is directly related to the duration of the initial ischemic insult. From the clinical standpoint, several authors have described the delayed recovery of cardiac function either after

thrombolytic therapy [5-7] or during and after percutaneous transluminal coronary angioplasty (PTCA) [8] to support the clinical existence of "stunning". From the experimental standpoint, data exist which demonstrate that periods of brief (less than 20 minutes) experimental coronary occlusion result in a functional deficit which only gradually resolves, taking from several hours to several days to fully recover depending on the duration of the initial insult [9].

Another concept that has both clinical and experimental support is that of "hibernating myocardium." This term was first introduced by Rahimtoola in his 1985 summary of data from three large multicenter randomized clinical trials of coronary artery bypass grafting (CABG) surgery for chronic stable angina [10]. This term was introduced to describe the situation in which:

> "...there is a prolonged subacute or chronic stage of myocardial ischemia that is frequently not accompanied by pain and in which myocardial contractility and metabolism and ventricular function are reduced to match the reduced blood supply."

In contrast to the concept of "stunning", hibernation is thought to represent a balance between flow and function. Bristow proposed that myocardial ischemia is a regulated process which serves "...to protect the anatomic and physiologic integrity of the cardiac cell" through a down-regulation of function and re-establishment of a metabolic balance [11]. Ross extended this concept when he emphasized the role of regional, as opposed to global ischemia in describing how flow and function are highly coordinated [12]. Clinical examples have served to illustrate this phenomenon in patients who are either post-CABG in whom functional recovery occurs with revascularization [13], or who demonstrate enhanced myocardial function with inotropic stimulation despite the presence of flow-limiting coronary stenoses (i.e. contractile reserve phenomenon) [14]. Although experimental models of myocardial stunning have been easy to generate, developing models of hibernation has proven more difficult. Models by Matsuzaki and Edwards using the in vivo dog heart [15, 16] and Liedtke using the extracorporeally perfused pig heart [17] have approached hibernation by looking at the flow function relationship in response to short-term reductions in coronary perfusion.

Need to Assess Function

Central to the concepts of both "stunning" and "hibernation" is the assessment of cardiac function. Determination of function can be divided into (1) measures of global function and (2) measures of more regional function.

Measures of purely global function center around the hemodynamic performance of the heart. One of the most basic measures of global function is the maintenance of forward flow of blood through the heart into the great arteries. This is typically measured as the cardiac output expressed as (liters of blood)/minute or cardiac index ($l/min/m^2$), which is the cardiac output corrected for the surface area of the individual. A second global index of cardiac function is the stroke volume, which is the difference in ventricular blood volume between end-diastole and end-systole. A third related measure of global ventricular function is the ejection fraction of the ventricle, defined as the stroke volume divided by the end-diastolic volume. These load dependent measures of function are not capable of providing information about ventricular function at the regional level since they represent the total efforts of all portions of the ventricular chamber.

Methods which assess both global and regional function, are also available. First, the use of echocardiography (ECHO) in the clinical and experimental setting to assess function has provided valuable information regarding (1) global performance as assessed by the ejection fraction, (2) regional wall motion, and (3) wall thickening [18-20]. This technique is advantageous because it is non-invasive, relatively inexpensive and expeditious. Second, equilibrium and first pass radionuclide ventriculography (RVG) at rest and with exercise is useful for both the detection of regional and global wall motion abnormalities and determination of left ventricular ejection fraction with increased reproducibility over ECHO. Finally, the use of left ventricular contrast angiography to assess wall motion provides yet another means to assess left ventricular function.

On the forefront of cardiac imaging today is the use of either (1) gated magnetic resonance imaging for the high resolution detection and tracking of regional wall motion and (2) cine-computed tomography which also provides for high resolution detection of regional wall motion and chamber volumes with the caveat of radiation exposure to the patient [21].

Inotropic Manipulation of Function

Inotropic stimulation in conjunction with analysis of regional or global function has been useful for the estimation of myocardial viability. Inotropic

agents (e.g. isoproterenol(ISO) and dopamine (DOPA)) have as their primary route of action, stimulation of beta-1 receptors in the heart. These receptors modulate the contractile and chronotropic state of the heart [22]. The use of these inotropic agents has proven to be most useful clinically to not only maximize cardiac function in a variety of settings, but also as a diagnostic tool to detect the presence of contractile reserve as a marker a cardiac viability [14, 23-25].

Further work in the experimental setting has examined the role of either ISO or DOPA stimulation in the setting of experimental "stunning" [26-28], and low-flow ischemia [25, 29, 30]. In these experimental settings however, inotropic stimulation (ISO>>>DOPA) was occasionally found to paradoxically depress perfusion and function in an area distal to critical coronary stenosis, presumably due to the induction of ischemia potentially related to the strong chronotropic effects of these agents. Inotropic agents have since been modified to provide the maximal inotropic stimulus while attempting to avoid the chronotropic, arrythmogenic, and vascular properties. In 1975, Tuttle an Mills introduced dobutamine (DOB), which had been chemically derived form isoproterenol [31]. Dobutamine has since found its way into a number of clinical uses, including: (1) the setting of acute myocardial infarction to improve or maintain adequate cardiac function [32, 33] (2) the setting of chronic progressive coronary disease and heart failure [23, 34, 35] and (3) the setting of non-invasive cardiac imaging with ECHO and or nuclear cardiac scanning to detect ischemia and/or assess viability [36-38, 99]. In contrast to ISO , in experimental models of infarction and "stunning", DOB has been found to consistently augment function in ischemic regions [25, 30, 39-41] . Thus, it is felt that dobutamine may be the preferable inotropic agent to maintain function and, when used in conjunction with various cardiac imaging procedures, provide useful diagnostic information.

Experimental Approaches to Function

There exists experimental approaches to function which permit a higher resolution approach to cardiac function than techniques discussed thus far. Among the most widely applied of these techniques are (1) the use of two paired ultrasonic crystals to examine wall thickening and/or segment shortening and (2) the use of a single epicardial Doppler crystal technique to obtain wall thickening data.

The ultrasonic two-crystal technique measures dimension by sensing the time required for a sound pulse, which is generated by one of the transducing crystals, to traverse the medium (myocardium) in which it is applied, and be received by the second crystal. To sense the distance between the two crystals, the time required for the sound pulse to travel from one crystal to the other is divided by the speed of sound through the intervening tissue (i.e. $x(dist) = (transit - time)/(transit - speed)$). This technique can be applied in one of two ways. First, both crystals can be implanted at the same depth in the myocardial wall along any of the cardiac axes to measure segment length changes during the cardiac cycle. Second, it is can be used to measure wall thickening at any depth of the myocardial wall by simply placing one of the crystals at a given depth in the myocardial wall, and placing the other on the epicardial surface. Thus, any displacement which takes place across between the two crystals during the cardiac cycle will represent the change in wall thickness. The potential advantages of this technique lie in its ability to detect (1) absolute distances of either segment length or wall thickening and (2) measures of wall thickening at multiple regional locations at the same time. The disadvantages of the two crystal technique are: First, to function correctly, the crystals must be properly aligned to achieve optimal signal transmission and reception. Second, the implantation of the crystals, up to 2 mm in diameter is traumatic to the cardiac wall and may distort the local fibers in such a way as to make measurements on absolute dimension unreliable [42].

A more recently developed technique to assess myocardial thickening is based on the pulse-echo mode of operation common to the two crystal method described above. This method, however, uses a single epicardial crystal, functioning as both transmitter and receiver by means of an adaptation of the pulsed Doppler theory of operation originally applied to sense blood flow velocity. The Doppler effect is based on the fact that "When an emitted sound beam is reflected from a moving target to a stationary receiver, the frequency of the received echo signal if different from the frequency of the original emitted signal" (i.e. the frequency is Doppler shifted) [43]. The single epicardial based crystal has a variable "range-gated sample volume" which allows the operator to sample the Doppler shift produced at any layer across the myocardial wall.

By (1) measuring this Doppler shift in frequency produced by the movement of myocardial layers passing back and forth through the range

gated sample volume, and (2) keeping track of the direction and motion of these displacements and integrating the velocity of movement, one can reconstruct the displacement of myocardial layers at the preset sample depth.

The advantages of this technique are multiple. (1) The crystal is applied without trauma to the myocardial wall, only three to five superficial sutures being required to secure it. (2) No alignment is required with a second transducing crystal. (3) Ease of application is greater since only one crystal need be applied. (4) Perhaps most importantly, this technique allows for the range-gated sample volume to be advanced stepwise across the myocardial wall to measure wall thickening discretely at various depths. It is this application of the technique which is being utilized in this thesis project to allow for the measurement of cardiac work on a sub-transmural basis.

The major disadvantage of the technique is the fact that, in contrast to the two crystal method, the absolute displacement in millimeters cannot be determined since only dynamic changes in wall velocity are being measured. This technique has been validated against the two crystal technique by placing the Doppler crystal on the epicardial surface of the heart and positioning a standard ultrasonic crystal within the myocardial wall opposite the first crystal. The intra-myocardial crystal was then connected to a module designed to receive the Doppler pulse emitted by the epicardial crystal. Thus, simultaneous measurements could be obtained via either (1) the single epicardial crystal method or (2) by the two crystal method using the same epicardial crystal this time, however, as the transmitter in a dual crystal setup. The waveforms and calculated thickening fractions were found to compare favorably between the two methods under conditions of normal perfusion and cardiac ischemia [42, 44].

This Doppler based method has since been applied experimentally to a model of "stunned" myocardium [45, 46] and clinically to monitor cardiac function in patients who are undergoing cardiac surgery [47]. The successful use of this technique to assess thickening in these situations indicates the value of this method in both the clinical and experimental setting.

Assessment of Transmural Function

One of the key applications of the above techniques has been the examination of the contractile function across the myocardial wall. Sabbah was first able to demonstrate using the two crystal technique that the inner half of the myocardial wall undergoes substantially more thickening ($\tilde{}$ 4:1)

than the outer half of the wall [48]. When Hartley first proposed the Doppler based method, he suggested that thickening was actually uniform across the myocardial wall [42]. However, later work by Zhu et al. using the same Doppler technique came to the conclusion that contractile function was in fact, nonuniform, with the endocardium thickening to a greater extent than more superficial layers [44]. This transmural gradient in contractile function has been supported by other authors using either the two crystal transit time technique [49, 50] or pulsed Doppler epicardial crystal technique [16]. It was demonstrated that under conditions of non-transmural ischemia produced by partial coronary occlusion, a dissociation of myocardial flow and function may occur in the epicardium [16]. This type of transmural analysis of function has given new insight into the contractile process with the promise of providing a better understanding of how contractility is regulated under changing conditions of supply and demand.

Importance of Flow

To fully address the concept of transmural function, one needs to discuss the role, regulation, and distribution of myocardial perfusion. On the simplest level of understanding, function cannot be sustained in the absence of blood flow. In the case of the in vivo working heart, this blood flow requirement is quite substantial. For an organ which weighs about 0.2% of body weight, it uses about 4.0% of the total body oxygen consumption which it extracts at a rate of 65-85% from the blood which passes through it [51]. To maintain this tremendous demand for blood, the coronary circulation has an elaborate system of autoregulation whose ultimate goal is to maintain perfusion under a wide range of conditions in sufficient quantity to provide the oxygen required for normal cardiac function despite wide variations in demand. The inotropic agents, which are known to augment function and therefore demand, have been shown to produce parallel increases in perfusion across the ventricular wall as myocardial work and oxygen consumption increase, as long as coronary autoregulation is intact [51].

Methodologic Approaches to Flow

The documentation of myocardial flow in the laboratory setting has been extensively studied. It has now become a standard practice to assess myocardial flow using the radioactive microsphere method first proposed by Rudolph and Heymann [52]. Briefly, this method involves the injection of a suspension of radiolabeled particles into the left atrium, to ensure adequate

mixing with blood, while simultaneously withdrawing a reference sample from the peripheral circulation. The reference sample is drawn at a known and constant rate. By subsequently comparing the counts in the reference sample with the counts in the myocardial sample, the myocardial flow can be determined. It has been shown that the microspheres are trapped in the small terminal vessels in the myocardium where they remain fixed without disturbing the native circulation. Furthermore, the microspheres are distributed to all organs in proportion to the regional blood flow that they receive [53, 54].

Markers of Function

The role of transmural perfusion and function has been extensively studied in a wide variety of experimental settings. In 1963, several articles were published which looked at the oxygen consumption, as an independent marker of myocardial work, and global coronary blood flow in a variety of canine models. The results of these experiments were indeterminate, as some investigators documented parallel changes in oxygen utilization with changes in coronary blood flow [55-57], while others did not [58, 59]. Work by Daniell in a canine model looked at the role of global flow reductions on both oxygen consumption and contractile force as measured with an epicardial strain gauge. This study reported a significant correlation between the coronary flow and both contractile force and oxygen consumption [60].

Later work by other investigators looked at the relationship between wall thickening as a marker of function and transmural flow was able to discern that more specifically, the blood flow to the endocardium correlates best with transmural function [16, 61-65]. These studies provide evidence that, while flow and function may be closely matched under normal conditions, regional dissociation between these two variables may exist when examined transmurally under conditions of ischemia.

Pressure-Volume Analysis

A third line of investigation into functional markers began with Suga in 1980 [66] with the use of the area traced by an X-Y plot of changing left ventricular pressure vs. changing left ventricular volume (P-V Diagram)(Figure 1). The pressure-volume area (PVA) inscribed by this diagram represents the total mechanical energy generated by a cardiac contraction. This includes both external work the heart does to generate forward movement of blood and potential energy which is stored as elastic

energy in the ventricular wall [67]. This potential energy can be used to contribute to the mechanical work under certain conditions [68]. The external mechanical work that the ventricle performs during a contraction is represented by the area inscribed by the counter-clockwise rotating lines of isovolumetric contraction/relaxation phases and the ejection/filling phases of the cardiac cycle [67]. The initial and subsequent studies were able to demonstrate that the PVA was linearly related to the oxygen consumption of the left ventricle under a variety of conditions [67, 69, 70].

Further analysis of the pressure-volume relationship revealed that by tracking the end systolic point in the P-V diagram under different loading and contractility conditions, a relation could be derived which was called appropriately, the End-Systolic Pressure Volume Line whose slope, (E_{max}), was found to be a powerful index of contractility [67, 69]. The use of various end-systolic based indexes have since been applied in different experimental settings for comparison. These include the development of end-systolic pressure-length [71, 72], left ventricular dimension-wall thickness [73] and stress-strain indexes [72]. The above indexes have been found to be comparable under most conditions for the accurate assessment of contractility.

Pressure-Length Analysis

The use of the PVA to measure cardiac work and predict oxygen utilization can only serve as a global index since it depends on the pressure and volume within the ventricular cavity. It fails to provide independent information about function and work at the regional level. The earliest attempts to assess regional function via loop analysis came with Tyberg in 1973 with the development of the clockwise rotating pressure-length loop generated using an epicardial mercury-filled silastic length gauge [74, 75]. Their analysis concluded that the area inscribed by this loop represented the mechanical work produced by a given cardiac segment during the cardiac cycle. Furthermore, by analyzing the morphometrics of these loops under ischemic conditions, information could be derived about the temporal sequence of contraction at various regions in the heart . The onset of ischemia was heralded by systolic lengthening with a sharp decline in the area of the pressure-length loop and actually reversal of the rotation of the loop. With severe ischemia, the ischemic segment was found to stretch passively during ventricular systole, providing evidence that the energy generated by the non-

ischemic segments was being dissipated into the ischemic segment (See Figure 2) [75].

A more recent investigation by Vinten-Johansen examined the relationship between the MVO_2, transmural segmental work and segment shortening (SS) after repetitive occlusion-reperfusion periods in the dog using the pressure-length loop. These authors noted a sharp decline in SS and pressure-length loop area with LAD occlusion, although a positive loop area (i.e. positive segmental work) was still generated despite akinesis and even dyskinesis in the segment. In addition, the MVO_2 declined but did not go to zero despite the profound changes in SS. These findings were taken as evidence that the discrepancy between SS and MVO_2 is partially due to the persistent development of segment work by the ischemic segment [76].

In 1991, Safwat et al. generated pressure-length loops using the two crystal ultrasonic technique to obtain their segment length data. In this analysis, the loops were analyzed with reference to both the end-systolic and end-diastolic time points (Figure 3). Three distinct periods were delineated within the loops: these were (1) the effective shortening area (ESA) occurring during systole (2) the post systolic shortening (PSS) area and (3) the segment lengthening area (SLA) occurring in early diastole. They concluded that only the effective shortening area was sensitive to ischemia, even more so than the total loop area [77]. A novel clinical application of the pressure-length loop has also been described whereby changes in segment length were obtained form left ventriculograms using a radial analysis to detect centripetal movement of the endocardial surface [78].

In an attempt to overcome the difficulty in measuring segment length in the clinical setting, Nakano et al. introduced a mathematical means to assess regional work which incorporates the wall thickness. The equation derived was $RWM = -\int \sigma d[\ln(1/H)]$, where $\sigma =$ stress as defined by P x D/4H, P=ventricular pressure, D=ventricular diameter and H= wall thickness, both of these dimension parameters being determined by ECHO. This technique has been validated in an animal model and was shown to reliably provide information about the regional work in both normal and coronary artery disease patients.

Hypothesis

Few investigators have thus far been able to relate the three variables of (1) contractile function, (2) myocardial perfusion and (3) cardiac

metabolism on the regional level with much success. This project was designed to gain further insight into the regional interrelationship of these variables. The Doppler based epicardial crystal technique of measuring sub-transmural myocardial thickening will be employed to generate left ventricular pressure-thickening loops as a novel approach to determining regional work. The area of the pressure-thickening loop will be related to flow, oxygen metabolism, and hemodynamic parameters of function at the transmural level and then subsequently at each level of the myocardial wall (i.e. endocardial, midwall, and epicardial) by relating the changes in work to the changes in flow. It is hoped that the ability of the Doppler technique to interrogate discrete layers across the wall will allow for the first time, the assessment of work on a sub-transmural basis with both accuracy and reproducibility. We propose to test this hypothesis in a normal canine model with graded dobutamine stress to examine work under different levels of inotropic stimulation.

Materials and Methods

Surgical Preparation:

Fasted mongrel dogs of either sex, weighing between 40-50 pounds were pre-medicated with atropine (0.07 mg/kg) and ketamine (10 mg/kg), then given by rapid intravenous bolus, sodium thiamylol (20 mg/kg) to induce rapid anesthesia. The animals were immediately intubated by direct laryngoscopy and ventilated on a pressure ventilator with a tidal volume of 20-25 cc/kg. Anesthesia was maintained with a 70:30 N_2O:O_2 mixture with halothane (.5-1.5 %) to a level at which (1) the eye blink response was abolished (2) no response was noted with surgical incisions and (3) no resistance to the function of the ventilator was observed.

The animals, once fully anesthetized were instrumented as follows. The limb leads of the electrocardiogram were placed to monitor the electrocardiogram. Bilateral groin dissections were performed to expose both femoral arteries and one femoral vein. A pair of 8F stiff-walled catheters were placed in one femoral artery, and a third catheter was placed in the other artery. An additional catheter was placed in a femoral vein to facilitate fluid administration. One 8f catheter from each femoral artery was reserved for arterial withdrawal during the administration of radiolabeled microspheres for flow, the third being used to monitor systemic pressure. A ventral midline abdominal incision was made to gain access to the urinary bladder for subsequent catheterization. The left neck was dissected for isolation of the external jugular vein and left common carotid artery. An introducer was placed in the common carotid artery to allow for the retrograde passage of a high fidelity Millar® micromanometer catheter to a sub-aortic valve position for measurement of left ventricular pressure and dP/dt. A 6f catheter was placed retrograde into the coronary sinus via the external jugular vein and a Swan-Ganz catheter was placed by the same route into the pulmonary artery to facilitate monitoring of body temperature, right atrial pressure and cardiac output by the indicator dilution method.

A left thoracotomy was then performed via the fifth intercostal space to expose the heart. The pericardium was opened and the heart suspended by a pericardial cradle. The left lung was retracted using an unfolded 4x4 gauze to facilitate access to the heart. A silastic catheter was placed into the left atrium via the left atrial appendage for the administration of radiolabeled microspheres and monitoring of left atrial pressure.

The proximal left anterior descending (LAD) coronary artery was dissected free, taking care to not disturb any septal branches, above the bifurcation of the second major diagonal branch to allow for placement of the Doppler flow probe and snare occluder.

Finally, Doppler thickening crystals were sutured to the epicardial surface in both of the regions supplied by the LAD and left circumflex coronary artery (LCX) using three to four 6-0 sutures penetrating the epicardial surface to a depth of 0.5-1.0 mm.

Theoretical Considerations of Doppler Based Method

As measurement of both proximal LAD flow and myocardial thickening in this animal preparation are based on the Doppler principle, the theoretical foundation of this technique will now be addressed.

The Doppler effect, as stated earlier, depends on the change in frequency of an emitted sound pulse produced by a moving object, which is detected by a stationary receiver. In the special case where a single transducer acts as both emitter and receiver, an equation exists which describes the relation between the velocity of the moving object and its Doppler shift:

$$V = (\Delta f \times c) / 2 \times fo \times (\cos \alpha) \quad \text{(equation 1)}$$

Where fo=transmitted frequency (Hz), V=velocity of the reflector (m/sec), c=speed of sound in the medium (m/s), α= angle between the direction of the emitted sound beam vector and velocity vector of the reflector and Δf=change in frequency produced by the moving reflector. For the flow probes used in this experiment, the angle α is fixed at 45 degrees by mounting the Doppler crystal in the silastic and wax housing which fits around the vessel. Since f_o = 20 Hz and the velocity of sound within the vessel is constant at 1500 m/s, then by substitution equation 1 becomes:

$$V \max(cm / \sec) = 5.3 \times \Delta f(KHz) \quad \text{(equation 2)}$$

The Doppler flow probe operates by emitting pulsed bursts of sound separated from one another by 16 usec into the blood vessel where they are reflected by the moving blood cells and received at a Doppler shifted frequency back at the probe. A useful means to describe the distance between transmitted pulses is to use the inverse of the period, commonly referred to as the Pulse Repetition Frequency (PRF) (i.e. PRF = $(.016 \text{ sec})^{-1}$ = 62.5 KHz). The time required for the sound echoes to be received is described by the equation:

$$t = 2 \text{ x } (d/c) \quad \text{(equation 3)}$$

Where t = time delay (sec), d = distance between the transducer and the reflector (m), and c = speed of sound in the medium (1500 m/sec). The receiver selectively samples the echoes received from within a "sample volume", which is a 1 mm^3 sensitivity region produced by the crystal. Echoes are sampled for a period of time whose length is defined by adjusting the "range-gate delay." For example, adjusting the range gate delay will move the sample volume to various positions across the vessel wall, thus proportionately changing the period of time during which echoes are received to allow for selectively sampling of flow at various vessel positions. The echoes which are received by the probe are then amplified and compared in phase and frequency to that of an internal reference oscillator which operates at the acoustic carrier frequency (f_o) of 20 MHz. The 20 MHz acoustic frequency chosen for this system, has been found to balance the tradeoff between the high acoustic scattering of blood cells which is proportional to the fourth power of frequency and the acoustic absorption of blood which also increases with frequency. Further, at 20 MHz the signals reflected from blood are strong enough to allow for the flow probe to sense velocity at distances from 1-10 mm from the crystal face, well within the range of normal epicardial vessel diameters. Since blood flow is typically expressed as ml/min, and not m/sec, a mathematical means to convert velocity into flow was developed by Hartley [79]. Under ideal conditions, flow is described by the equation:

$$Q(ml/\min) = (Vavg(mm/\sec) \times Area(mm^2)) \times 60 \quad \text{(equation 4)}$$

Where Vavg = average velocity of flow across the vessel wall. However, since cross sectional area is not readily determined <u>in vivo</u>, it was determined that under conditions of laminar flow with a parabolic velocity profile, Vavg = Vmax/2. By substitution, the flow equation then becomes:

$$Q(ml/\min)/\Delta f(KHz) = (5.3 \times Area(mm^2))/2 \quad \text{(equation. 5)}$$

By setting the Area = $d^2/4$ where d = internal vessel diameter estimated by the size of appropriately fitting flow probe, one derives the final equation for flow:

$$Q(ml/\min)/\Delta f(KHz) = 1.25 \times d^2 \quad \text{(equation 6)}$$

This method has since been validated with against timed collections of effluent blood with a strong linear relationship being found to exist.

To ensure proper function of the flow probes, several precautions need to be taken. First, adequate fit of the flow probe around the vessel ensures that the angle between the embedded Doppler flow crystal and vessel axis remains

constant at 45 degrees. Proper fit also ensures that the vessel diameter will be estimated correctly for use in the velocity to volume calculation. Flow probes are supplied in 0.5 mm increments with internal diameters of 2.0-3.5 mm. Second, the sample volume needs to be positioned in the center of the vessel axis to ensure that maximal blood flow velocity is being sampled. As stated earlier, assuming conditions of laminar flow with a parabolic velocity profile, this position is easily determined as that at which the signal obtained has the greatest amplitude. Third, to avoid deterioration in signal quality from non-laminar blood flow, the probes need to be placed at the most proximal position on the vessel, typically proximal to the second major diagonal branch and snare occluder. The final step to ensure proper function is correct calibration of the probe by systematically applying a known Doppler shift frequency from which the flow instrument is able to register the appropriate voltage reading.

Working from the same theoretical framework as Doppler based flow measurement, Hartley developed the technique to measure wall thickening [42]. The Doppler probe consists of a 4 mm disk of 10 MHz piezoelectric crystal which has been attached to a circular piece of Gortex® graft material, used to secure the probe to the epicardium. The probe operates much like the flow probe, by using pulsed sound waves directed perpendicular ($\alpha = 0^0$ from equation 1) to the myocardial wall to detect the Doppler shift produced by the movement of various myocardial layers within the sample volume during the cardiac cycle. The range gated sample volume is adjusted as before to allow for interrogation of the various layers across the wall, at depths ranging form 2-40 mm. The crystal operates at an ultrasonic frequency of 10 MHz with a PRF of 4 KHz (250 usec separation). By comparing the echoes produced by the myocardium with those of two internal reference oscillators, the phase difference is used to convert back and forth movement in time into up and down motion in voltage at the given range delay. In essence, the circuitry electronically integrates the velocity of myocardial wall movement to determine displacement.

This method does not depend on the ability to track a discrete interface, rather, displacement is measured at a fixed depth. Thus, within the sample volume, the myocardial layers present at any given time change throughout the cardiac cycle. Layers within the sample volume at end-diastole tend to be deeper than those seen at end-systole since the wall has thickened. Since no

layer is tracked, the starting point for the phase detection is arbitrary, thus it is not possible to measure the absolute thickness, only the relative excursion. Furthermore, the final output location along the thickening axis, as it appears on the chart recorder bears no relation to the actual thickness of the wall.

The variable range gate delay is used to set the time delay (3-50 usec) at which the phase of the signal is sampled. Since the echoes produced by the myocardium are relatively low frequency when compared to those of blood flow, the audio echo signals are limited to a band extending from 1 Hz to 1 KHz, thus allowing velocities from .075 mm/sec to 7.5 cm/sec to be sensed. For comparison, blood velocities usually range from 1 to 100 cm/sec with an associated audio band of 100 Hz to 10 KHz [42, 43, 79]. The sampled phase changes are recorded such that movement toward the probe advances an electronic counter, while movement away subtracts from the counter. The real time output from the counter is then fed through an analog to digital converter which produces the final voltage output which is calibrated to a millimeter displacement. The resolution of the system allows for displacements as little as .02 mm to be detected.

To measure wall thickening quantitatively, the % thickening fraction (%TF) of the various myocardial layers is determined. By the classic two crystal ultrasonic technique, %TF is expressed by the following equation:

$$((EST - EDT) / EDT) \times 100 \quad \text{(equation 7)}$$

Where EST = end-systolic thickness and EDT = end-diastolic thickness. In this preparation, since absolute thickness is not directly possible, a mathematical means was developed by Hartley [42]. By knowing the value of range gate delay (R) in mm, and the total systolic excursion (SE) of thickening in mm, %TF is described by the equation:

$$\%TF = (e^{(SE/R)} - 1) \times 100 \quad \text{(equation 8)}$$

Operation of Doppler Thickening System

As stated earlier, thickening crystals are placed in both the LAD and LCX territories for the collection of data. The proper range gate delay, is determined by gradually advancing the range gated sample volume until the blood pool is detected by a sharp change in the audio signal. The sample volume is then brought back to a position where the quality of the signal is consistent throughout the cardiac cycle. The maximal depth that the Doppler crystal (as well as the dual crystal ultrasonic crystal technique) is able to sample thickening at, has been estimated to be 85% of the total wall thickness

[16,94]. As demonstrated in Figure 4, this depth is considered to represent the transmural thickening. The total range is then divided in thirds, thus allowing signal sampling at two other positions besides the transmural point. Since the crystal measures thickening between the level of the sample volume and the crystal itself, the three positions across the myocardial wall will represent thickening of the: (1) transmural (Tm) or full wall thickness, (2) outer two-thirds (Out 2/3) of the wall and (3) outer one-third (Out 1/3) of the wall. To avoid placing the crystals, especially the one situated in the LCX territory, over a papillary muscle, the range gate at which the blood pool is encountered is tracked at various positions within the territory. Papillary muscles are easily determined as positions on the myocardial wall at which the blood pool location is deeper than expected (e.g. greater than 14 mm). Once the crystals are positioned correctly, both the range and thickening are electronically calibrated to ensure appropriate function.

Computer Data Acquisition

All experimental data are recorded using an eight channel computer based data acquisition program referred to as DATAFLOW (Crystal Biotech, Holliston MA). The hardware includes a multichannel interface module (VF-1, Crystal Biotech) whose output is linked through an analog to digital (A/D) converter to a 486(25 Mhz) Computer (Gateway 2000). An oscilloscope is used to give a visual representation of the range outputs from both thickening crystals and the flow probe. Dataflow is able to interpret the digital output of the A/D converter into the appropriate units and reconstruct the channel outputs in real time. In addition, Dataflow computes a variety of statistics in real time for each channel (e.g. mean, max., min, +/- derivatives etc...) (See Figure 5).

Dataflow collects the data from a total of eight channels during the course of each experiment: (1) LAD flow output from the 20 MHz pulsed Doppler module in VF-1 (PD-20; Crystal Biotech) (2) LAD Thickening from the pulsed Doppler dimension module (DMM-10; Crystal Biotech) (3) Left Ventricular Pressure (LVP) from the Millar Micromanometer module (Millar Industries) (4) LAD Thickening Range also from the DMM-10 module (5) ECG for heart rate from the limb leads of the electrocardiogram (6) Aortic Pressure for both systolic and mean pressure from a fluid filled pressure transducer output (7) LCX Thickening from the second DMM-10 on the VF-1 and finally (8) LCX Range from the same module. Dataflow has built in

derivation of the first derivative of left ventricular pressure (dP/dt) which is displayed simultaneously with the LVP. All eight channels above are also directed into an eight channel pen recorder for hard copy record.

Dataflow provides the ability to save large amounts of data in two different formats during the course of a given experiment. The program is first able to create a trending file of all channels at user specified intervals of 10-60 sec. Second, the user can perform manual saves to capture up to eight channels of data at specific time points in the experiment. These data are stored at intervals of .00221 sec for a total of about 5 seconds to give 300-2400 data points (1500 for this preparation). These manual saves provide the raw data for subsequent analysis.

Other data not recorded through Dataflow includes: Cardiac Output using the Swan-Ganz catheter and Cardiac Output computer (Edwards Laboratories, New York, NY), body core temperature from the Swan-Ganz catheter, arterial blood gas data every 45-60 min, left and right atrial pressures and metabolic data for oxygen content.

Myocardial Blood Flow Determination

Regional myocardial blood flow is determined using the radiolabeled microsphere referenced withdrawal technique introduced by Rudolph & Heyman in 1967 [52]. Microspheres (12 um diameter), supplied by DuPont were pre-labeled with the following isotopes: Sn-113, Sc-46, Ru-103, Cr-51 and Nb-95. Prior to injection, the dose of microspheres to be given (average >2 million) are decay corrected to ensure that the radioactivity injected for each flow determination is comparable. The microspheres are mixed with saline, vortexed and flushed between two syringes via a three way stopcock to ensure an even distribution without microsphere aggregates.

Prior to injection of the microspheres, the withdrawal pump connected to the two 8F femoral artery catheters is started to ensure the smooth return of blood. Once constant flow is established, the microspheres are injected into the left atrium over a 15-20 second period, followed by 5 cc of saline as a flush. The withdrawal pump continues at a constant rate of 5.68 cc/min for 95 seconds providing paired 9 cc samples of blood. Once complete, an additional 3 cc of blood from each catheter is withdrawn to ensure clearance of all microspheres from the catheter "dead space". It has been shown that no microspheres remain in the circulation 60 seconds after injection [54]. The 24

cc of blood is evenly divided among 16 vials and weighed in preparation for gamma well counting.

Post-mortem the heart is trimmed to separate the ventricles and septum from the rest of the heart. The ventricles are then divided into five (5) slices along the short axis from base to apex. The slices are then incubated in a solution of triphenlytetrazolium chloride (TTC) at 37 °C for 20 minutes to delineate any necrotic myocardium. The slices are photographed and the location of the thickening crystals are marked on an acetate template.

The visceral pericardium and any remaining fat are trimmed in preparation for gamma well counting for the determination of regional blood flow. The short axis slices are then divided into eight evenly spaced radial segments, with each segment then being divided into thirds to separate the endocardium, midwall and epicardium. Each slice is placed in a numbered vial (1 to 96), weighed and counted in a multichannel gamma well counter (Cobra Systems). Separation of the activity for each radiolabeled microsphere by specific energy windows was performed according to the method of Heymann [54] with the appropriate spill-up and spill-down corrections.

To determine the myocardial blood flow, the following formula was utilized [52]:

$$Q_m = C_m \times Q_{ref} / C_{ref} \quad \text{(equation 9)}$$

where Q_m=myocardial blood flow (ml/min), C_m=radioactivity in myocardial sample (cpm), Q_{ref}=reference withdrawal rate (ml/min) and C_{ref}=radioactivity in the reference withdrawal sample (cpm). Flow is then corrected for the weight of each myocardial sample so that final flow is expressed in units of ml/min/gm.

This technique provides the ability to assess flow at multiple time points during the course of single experiment. It has been shown that appropriately sized microspheres are permanently trapped in the microcirculation on the first pass without causing any hemodynamic compromise [54].

To facilitate the comparison of flow with the pressure thickening loops at the sub-transmural level, only those myocardial sectors which immediately surrounded the location of the crystals were used. This typically meant that five total sectors were used: (1) at the crystal (2) above and (3) below the crystal and to the (4) right (5) and left of the crystal.

Metabolic Data Processing

Using the temporally paired blood samples from the coronary sinus and femoral artery, the % saturation of hemoglobin (Hb) was determined using a hemoximeter (OSM2 Hemoximeter, Radiometer Copenhagen). The oxygen content of each sample was calculated using the Hb concentration and the constant 1.33 ml O_2/gm hemoglobin. The differences in oxygen content were then calculated between arterial and coronary sinus/AIV samples and multiplied by regional flow (taken form the five sectors described above) to measure the regional oxygen consumption (MVO_2).

Experimental Protocol: ***Normal response to dobutamine***

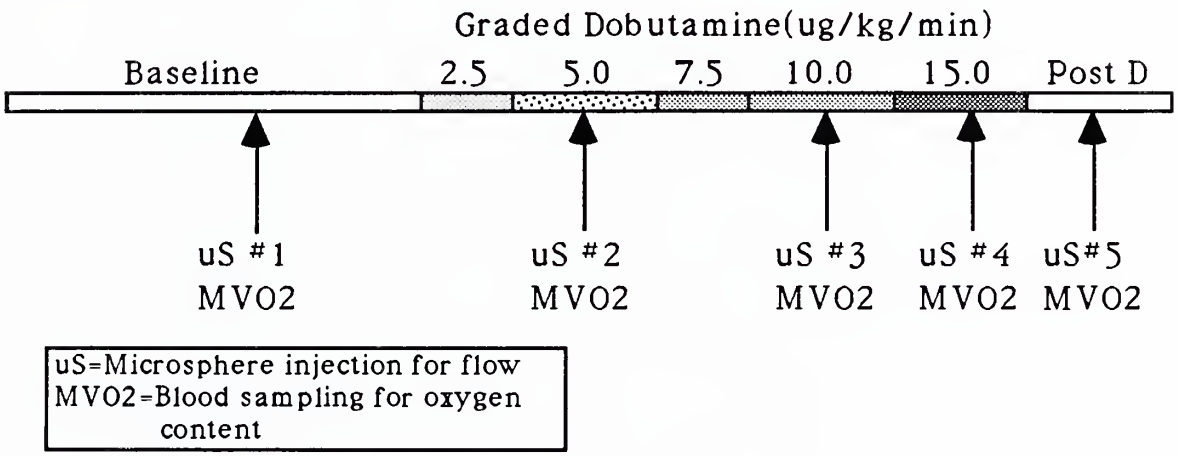

A) A 30-45 minute baseline period with injection of the first microsphere for regional flow determination.

B) Dobutamine, obtained as a stock solution (Dobutrex ®, Lilly) of 250 mg/20 ml (12.5 mg/ml) was diluted using sterile saline and injected into the left foreleg brachial vein using a digitally calibrated screw infusion pump to achieve precise infusion rates.

C) Graded dobutamine infusions were done @2.5 ug/kg/min (D2.5) for 10 minutes, @5.0 ug/kg/min (D5.0) for 15 minutes with injection of second microsphere for regional flow, @7.5 ug/kg/min(D7.5) for 10 minutes, @10 ug/kg/min(D10.0) for 15 minutes with the third microsphere for regional flow determination, and @15 ug/kg/min (D15.0) with injection of the fourth microsphere for flow.

D) A 15-30 minute period of observation after dobutamine (Post D) was concluded was used to monitor recovery and assess myocardial flow with the fifth microsphere injection.

E) The animals were sacrificed using a bolus of 2M KCL with subsequent excision of the heart. The heart was then prepared for gamma well counting as described above.

The following data (unless otherwise specified) was collected at 5 minute intervals during baseline, twice at each level of graded dobutamine and at two points during the 15 minute post dobutamine period.

(1) Hemodynamic measures: Heart rate, mean aortic pressure, right and left atrial pressure, left ventricular pressure with its first derivative (dP/dt), LAD Doppler flow, and cardiac output .

(2) Thickening data: Thickening and range data were obtained at the Tm position at the intervals specified above. In addition, thickening and range data was obtained at the Out 2/3 and Out 1/3 positions twice during baseline, once at each level of dobutamine and twice during the post dobutamine period.

(3) Metabolic measures: Blood samples for oxygen content were temporally paired to the determination of regional blood flow with radioactive microspheres.

(4) Arterial blood gas (ABG): ABG's were determined at intervals of 45-60 minutes throughout the experiment.

Derived Data

In addition to the hemodynamic parameters mentioned above, two additional hemodynamic indices were computed. (1) The pressure-rate (P-R) product defined as the product of peak aortic pressure and heart rate expressed as mmHg x beats/min. (2) The systemic vascular resistance was also calculated using the following:

$$SVR = ((MAP - RAP) \times 80) / CO \quad \text{(equation 10)}$$

Where MAP = mean aortic pressure, RAP = right atrial pressure and CO = cardiac output.

Data Processing for Pressure-Thickening Loops

All data processing was performed using Microsoft Excel® on the 486 25 MHz computer described earlier. Microsoft Excel® is a spreadsheet program which allows large amounts of data to be manipulated and plotted. The X-Y graphic plots of left ventricular pressure vs. thickening used to create the pressure-thickening loops were all generated using this program. The

following is a narrative description of the steps involved in processing of the data.

A. The raw hemodynamic data derived from Dataflow® consisted of the 1500 data points with an average of 6-9 complete cardiac cycles. This data was first downloaded into Excel® in the form a worksheet. Data analysis was restricted to the LAD and LCX thickening data and left ventricular pressure (LVP). Using Excel®, a automated program (i.e. a "macro") was written to calculate dP/dt for all 1500 data points using the following equation:
$$dP/dt(mmHg/\sec) = (LVP_{x+1} - LVP_x)/(time_{x+1} - time_x) \quad \text{(equation 11)}$$
Where x = an arbitrary point in time within the data file.

B. The thickening signal was first displayed using Excel® to ensure signal quality. Five full cardiac cycles were then selected based on the dP/dt using the point of initial upstroke as the onset of systole and the point immediately preceding the next initial upstroke as the end of diastole. In cases where five beats could not be used due to either insufficient number of beats per data set or compromised signal quality, the maximum number of possible beats were utilized.

C. The data contained within these five intervals for LADTH, LVP and LCXTH was copied to a new Excel® worksheet where it was rearranged into columns of thickening and pressure data for each of the selected beats using another macro written for this purpose.

D. Each of the separate thickening signals was then normalized to the minimum thickening value for each beat. Thus expressing each beat as a net excursion from its minimum value. This step was necessary to compensate for the variable position of the signals along the thickening axis. As discussed earlier, since the thickening signal position bears no relation to the actual thickness, the loops obtained prior to normalization could be centered on virtually any value. By normalizing, all loops were based on a zero point for consistency.

D. The average values for five normalized beats were then taken for LADTH, LCXTH, and LVP. dP/dt was re-computed based on the average LVP for the five beats and time interval between the data points.

E. X-Y plots were then made using Excel® for mean LADTH vs. mean LVP and for mean LCXTH vs. mean LVP to generate the pressure thickening loops, each representing the average of the five

averaged cardiac cycles.(See Figure 6) This process was repeated for each manual save, including those with data for transmural, outer 2/3 and outer 1/3 thickening during the course of each experiment.

F. The net systolic excursion was then calculated by taking the difference between the maximum and minimum thickening value during the systolic interval (where systole is defined by the initial upstroke of dP/dt to peak negative dP/dt) for each of the normalized beats. The average systolic excursion was then calculated for both the LADTH and LCXTH.

G. By using the average systolic excursion and Doppler range obtained from the original data file, the thickening fraction was then calculated using the formula (equation 8) derived by Hartley.

H. To calculate sub-transmural thickening fractions, the difference in systolic excursions was then taken such that Endocardial (Endo) = (Transmural)-(Outer 2/3); Midwall (Mw) = (Outer 2/3)-(Outer 1/3) and Epicardial (Epi) = Outer 1/3. The respective differences in the ranges were used in equation 8 to generate the respective %TF for each sub-region.

I. Each of the pressure-thickening loops which was generated was then planimetered three times using a SummaSketch® (Summagraphics) digital planimeter pad then averaged. The area of the loop was expressed in the square number of digital pixels occupied by the loop on the planimeter pad.

J. Similar to the approach to obtain transmural thickening data, differences in measured areas were then computed to generate the net area values for the Endo, Mw and Epi sub-regions.

Laboratory Responsibilities

All surgical responsibilities were divided among this investigator, Jonathon Alderman and QingXin Shi. Dr. Albert Sinusas was responsible for placement of the coronary sinus venous catheter and assistance with any technical problems encountered during the course of the experiment. Dr. Lawrence Young was responsible for processing of all metabolic blood samples. All data analysis, with the exception of operation of the gamma well counter and subsequent computation of regional blood flow, was performed by this investigator.

Statistical Analysis

All statistics were performed using Statview® 512, a statistical and graphics program for the MacIntosh computers. Correlations were expressed as the Pearson (r) correlation. Statistical significance (at least $p < .05$) was determined using a standard significance table with the appropriate degrees of freedom [80].

Results

A total of seven dogs were used for this study. Two of these animals were subsequently excluded from the data set: one secondary to a malfunction of the Millar® pressure catheter and the other for technical complications related to the surgical preparation. Of the five remaining animals, complete data sets are available for three animals. The other two animals lacked either complete metabolic or flow data sets. In addition, thickening and loop data from the LCX region needed to be excluded for one animal secondary to poor signal quality.

Hemodynamics(Table 1)

Summarized in Table 1 are the hemodynamic parameters during the experimental protocol. The heart rate, R-P product, maximal value of dP/dt, cardiac output and LAD flow as measured with the Doppler flow probe steadily increased with graded dobutamine dose. These hemodynamic parameters generally returned to values intermediate to those of the baseline and D5.0 when dobutamine was discontinued. The mean aortic pressure (mean AoP) responded differently with an initial increase up to D5.0 after which the mean pressure actually declined slightly with further increases in dobutamine. The mean AoP then returned to baseline 15 minutes after dobutamine was stopped. To further examine changes in the vascular tone during these studies, the systemic vascular resistance (SVR) was calculated. With graded dobutamine, the SVR steadily declined, from a value of 3708 +/- 242 at baseline to 1989 +/- 281 at D15.0.

Regional Microsphere Blood Flow (Table 2)

The regional blood flow at the Endo, Mw, Epi and Tm levels for both the LAD and LCX region are reported in Table 2. Throughout the study, the flow across the wall in both perfusion territories behaved identically with increasing dobutamine producing parallel increases in flow. In the post dobutamine period, however, flow decreased but failed to return to baseline levels. Potential explanations for this observation are offered below.

Thickening Data (Table 3)

A representative baseline LAD tracing of the thickening signals obtained at the Tm, Out 2/3 and Out 1/3 sampling locations are shown superimposed in Figure 7 to demonstrate how thickening increased progressively as the Doppler range was advanced from the epicardium towards the endocardium.

The data for the LAD and LCX territories at both the transmural and sub-transmural levels are summarized in Table 3. The %TF at all levels was found to initially increase with dobutamine, then plateau as dobutamine increased. The thickening fraction returned to baseline levels once dobutamine was stopped.

The %TF for the Endo, Mw and Epi exhibited a transmural gradient favoring the deeper myocardial layers in both territories throughout the experiment. With graded dobutamine, the %TF for the Endo and Mw tended to equalize in both the LAD and LCX regions, while consistently remaining higher than the %TF for the epicardium.

Pressure-Thickening Loop Area (Table 4)

Sub-transmural work was estimated by analysis of the pressure-thickening loop areas. The changes in these loop areas for both the LAD and LCX regions are summarized in Table 4. A typical LAD Tm (full wall thickness) pressure-thickening (P-T) loop at peak dobutamine is illustrated in Figure 6 . All area measurements of P-T loop areas are expressed in units of square pixels occupied on the digital planimeter pad described earlier.

There was a different response in the loop areas to dobutamine in the LAD and LCX regions. With graded dobutamine, the LAD Tm loop area, and therefore work, progressively increased with each level of dobutamine while the LCX Tm work plateaus after D 2.5. Further sub-transmural analysis demonstrated that: (1) Dobutamine greatly increased work when compared to baseline although in a nonlinear manner. (2) At all times, the work performed by the Endo and Mw was greater than that performed by the Epi. (3) At 15 minutes after dobutamine, work declined although did not return to pre-dobutamine levels in all animals.

Metabolic Data

The regional oxygen consumption (MVO_2)(ml O_2/min/100 gm) for the LAD perfusion territory was calculated as a independent metabolic measure of regional work. With graded dobutamine the MVO_2 increased steadily from 10.65 +/- 2.35 at baseline, to 11.18 +/- 1.03 at D5.0, 11.52 +/- 0.87 at D10.0, and

13.25 +/- 0.77 at D15.0. With the cessation of dobutamine, the MVO_2 declined towards baseline to a value of 9.20 +/- 0.80.

Loop Areas and Indices of Myocardial Work (Table 5)

To evaluate the use of the P-T loop as an index of work, correlations were sought between the Tm loop area in the LAD and LCX region and either the MVO_2 (LAD only), R-P Product, or maximal dP/dt. All data points were expressed as a % change from baseline in order to facilitate the incorporation of multiple animals into the same data set. These three variables were used to compare the P-T loop to both regional (MVO_2) and global (R-P product and maximal dP/dt) indices of work. As seen in Table 5, a fair ($r=.524$)($p<.05$) correlation exists between the LAD Tm loop area and regional MVO_2 (Figure 8 a). Comparisons between the Tm loop area and the hemodynamic indices of work revealed significant correlations between the LAD Tm loop area and both the P-R Product ($r=.648$)($p<.01$) and max. dP/dt ($r=.814$)($p<.01$)(Figures 8 b-c). Equally significant correlations were found between the LCX Tm Loop area and max. dP/dt ($r=.822$)($p<.01$) and P-R Product ($r=.917$)($p<.01$)(Figures 9 a-b).

Blood Flow Relations to Loop Area and Indices of Work: (Table 5)

The relationship between both LAD and LCX transmural flow was then compared, after normalization baseline as before, to the same three markers of function as above. In each case, there an excellent correlation found to exist between the LAD transmural blood flow with either the (1) MVO_2 ($r=.886$)($p<.01$) (2) P-R Product ($r=.912$)($p<.01$) or the (3) max. dP/dt ($r^2=.863$)($p<.01$)(Figures 10 a-c) and LCX transmural blood flow with both the (1) P-R product ($r=.901$)($p<.01$) and (2) max. dP/dt ($r=.871$)($p<.01$)(Figures 11 a-b). Transmural flow was also related to the area of the P-T loop area with significant correlations being demonstrated for the LAD ($r=.633$)($p<.05$)(Figure 10 d) and LCX ($r=.879$)($p<.01$)(Figure 11 c) territories.

To evaluate the P-T loop area as an index of change in sub-transmural work, comparisons were sought between microsphere flow and loop area at the Endo, Mw and Epi levels for both the LAD and LCX territory. Microsphere flow was used as the comparative index of work based on (1) the strong correlations noted between the transmural flow and both metabolic and hemodynamic indices of work and (2) the lack of appropriate metabolic and hemodynamic indices of work at the sub-transmural level. As shown in Table 5 and Figures 12 a-c, for the LAD territory, significant correlations between microsphere flow and loop area were noted only for the midwall and epicardial sub-regions,

with a non-significant positive correlation noted for the endocardial sub-regions: endocardium (r=.256)(p=NS); midwall (r=.572)(p<.05); epicardium (r=.681)(p<.01). In contrast, Table 5 and Figures 13 a-c demonstrate that for the LCX territory, significant correlations were noted only in the endocardial and epicardial sub-regions, with a non-significant positive correlation found for the midwall sub-region: endocardium (r=.917)(p<.01); midwall (r=.523)(p=NS); epicardium (r=.766)(p<.01).

Discussion

In this study, we have demonstrated that analysis of regional left ventricular pressure-thickening loops holds promise as a reliable index of changes in cardiac work. These loops were generated using a new Doppler based epicardial thickening crystal which provided for the ability to discretely sample the thickening at the level of the endocardium, midwall and epicardium. The transmural loop area was found to correlate significantly with transmural myocardial blood flow, MVO_2 and accepted hemodynamic indices of global myocardial work. In addition, strong positive correlations were found between the transmural flow and these same indices of work supporting the use of flow as an indirect index of work at the sub-transmural level. Finally, the Endo, Mw and Epi P-T loop areas were examined with respect to their sub-transmural blood flow where in general, significant correlations were noted. It is therefore the conclusion of this thesis that the left ventricular pressure-thickening loop may prove, with further analysis, to be a reliable index of changes in regional work at a level of analysis not previously available.

Loop Area Analyses with Comparisons to Indices of Work

Suga has extensively studied the use of the pressure-volume loop area (PVA) as an index of cardiac work by relating it to myocardial oxygen consumption [67, 69]. The correlation reported between these variables was higher (r^2=.98) than that reported in this study (r^2=.274). One potential explanation for this discrepancy is that the model used by Suga, in contrast to that used here, was that of an ex vivo canine-excised, cross-circulated heart where pressures and volumes could be precisely controlled. A second possible explanation lies in the fact that the pressure-volume analysis is by definition, a more global assessment of work than the P-T loops generated in this project. It is possible that the MVO_2 and work at the regional level (i.e. using the pressure-thickening analysis) may show local heterogeneity, the details of

which could be masked in measuring these variables at the global level (i.e. the pressure-volume analysis).

Recent work by Starling took the PVA analysis one step further by examining whether the use the PVA improves upon other hemodynamic based measures of myocardial work. Of relevance to this project was the finding that both the PVA and P-R product had a similar correlation to the MVO_2. Thus, it was concluded that the PVA did not improve on the other indices of myocardial work [70]. The relative importance of this type of global analysis using the PVA was thus called into question since it fails to provide more useful information than methods clinically available (e.g. calculation of P-R product).

Other investigators have approached the measurement of segmental myocardial work from a more regional level using the pressure-length (P-L) loop. Forrester et al. found a linear relationship between the area of the P-L loop and the stroke work suggesting that the area circumscribed within this loop was a valid index of segmental performance [81]. This type of validation was limited in that comparisons of work at the regional level were made to more global indices of cardiac function (i.e. the stroke work) [75].

Recent work by Vinten-Johansen compared the pressure-length loop area at the transmural level to both segment shortening and regional MVO_2 after repetitive occlusion-reperfusion periods in the dog. This study was one of the first to quantitatively compare the P-L loop area to a metabolic index of regional work. The authors noted a strong positive correlation between the stroke work (i.e. P-L loop area) and regional MVO_2, both of which remained elevated in the face of dyskinesis and/or akinesis in the involved segment. The study, therefore, came to the conclusion that continued segmental work was partially responsible for previously noted discrepancies between segment shortening and regional MVO_2 . While the goal of this study was not a validation of the P-L loop as an index of regional work, the good correlation with regional MVO_2 partially supports this hypothesis.

This thesis improves upon these earlier attempts using the pressure-length loop, by validating the use of the pressure-thickening loop against three independent markers of myocardial work. The first index to which the P-T loop was compared was the myocardial oxygen consumption (MVO_2). The MVO_2 has been shown to be linearly related to the inotropic state of the heart [82]. The findings in this thesis that the MVO_2 steadily increased with graded

dobutamine are in agreement with these earlier observations. This is not surprising based upon the strong β_1 properties of dobutamine which increase cardiac work through inotropic and, to a lesser extent, chronotropic effects [22]. The strong interrelation between cardiac work and the MVO_2 has made this index a "gold standard" for comparison for other indices of work.

The other two indices of work used for comparison in this study are related to the hemodynamic performance of the heart. First, the pressure-rate product depends on changes in both heart rate and systolic arterial pressure, both of which have been shown to positively contribute to oxygen consumption and therefore cardiac work [83]. Concern regarding the use of the P-R product to estimate the MVO_2 and therefore work in a canine model using halothane anesthesia was addressed by Rooke. He was able to demonstrate that the P-R product was indeed a valid index of estimation of myocardial work despite halothane anesthesia [84]. The third index utilized in this study was the maximal value of the first derivative of left ventricular pressure with respect to time. Again, this index was also found to linearly relate to oxygen consumption and work [82]. Based on these findings, we felt that the excellent correlations noted between the P-T loop area at the transmural level and these indices of work provided an empirical validation of our approach to regional work.

As alluded to earlier, the lack of both hemodynamic and metabolic information at the sub-transmural level led to the use of flow as the basis of comparison for the sub-transmural P-T loop areas. The significant correlations found at the transmural level between flow and the MVO_2, P-R product and maximal dP/dt indicate that in this preparation, flow behaved as an approximate index of work for comparison to the P-T loop areas.

Regional Differences in Loop Area vs. Flow Correlations

At the sub-transmural level of analysis we noted an inconsistent pattern of correlations between microsphere determined blood flow and respective loop area. Specifically, microsphere flow and loop area failed to reach statistical significance for the endocardium in the LAD and the midwall in the LCX territory. The most likely explanation for these unexpected findings relate to statistical uncertainty associated with the small sample size.

Numerous authors have shown that, under pathologic conditions, flow and thickening correlate best in the deeper myocardial layers , especially the endocardium. Under normal conditions however, one finds that flow and

thickening correlate in both superficial and deeper myocardial layers. This is true under a variety of experimental conditions including ischemia, exercise and atrial-paced tachycardia [61-64,87,93]. One would therefore expect that the pressure-thickening loop area, being derived from thickening data, would show the same relationship to flow. We are optimistic that with additional studies, this relationship will indeed hold true.

Regional Differences in Changes in Loop Area With Dobutamine

The results of this study would seem to indicate a different response to dobutamine between the LAD and LCX territories with respect to changes in the pressure-thickening loop areas. A priori, there would be no reason to expect a different response in one bed versus the other as both were studied under the same conditions. One explanation for this observation again lies in the small sample size used here. It is therefore possible, and to be expected, that with augmentation of study numbers, the observed responses to dobutamine would equalize.

A second potential explanation could be that there were subtle differences in signal quality between the LAD and LCX territories. Since the LAD and LCX pressure-thickening loops are generated using the same intra-ventricular pressure, any difference in signal quality could adversely affect the quality, and therefore the area of the loops. As the LCX Doppler crystal occasionally lies close the pericardial cradle, movement of the pericardium against the crystal may affect signal quality in that region. Any difference inherent to signal quality between the LAD and LCX regions should be borne out as more experiments are performed.

A third potential explanation may lie in the placement of the crystals on the epicardial surface of the left ventricle. The LCX crystal tends to be placed in a more basal position relative to the LAD crystal to avoid placement of the LCX crystal over a papillary muscle. There may be as yet undefined differences in contractile reserve between these crystal locations which could limit changes in the loop area with inotropic stimulation.

Regional Function Analysis

The use of the Doppler based method to assess myocardial thickening has several importance advantages when compared to the standard two-crystal transit time technique. To elaborate on those eluded to in the introduction, each will now be addressed separately.

The Doppler technique is less traumatic to the myocardium since each crystal is sutured only to the epicardium using a few sutures penetrating 0.5-1.0 mm into the wall. In contrast, implantation of the ultrasonic crystals requires a stab wound into the ventricle through which the crystal is tunneled into the wall. The crystal occupies a 2 mm^3 space within the wall producing both edema at the stab wound and secondary distortion of the local fibers. The effects of this distortion are impossible to quantitate and may adversely affect the accurate measurement of segment length and thickening.

The second and related advantage of the single crystal Doppler technique is that its proper function is affected less by changes in fiber orientation across the myocardial wall. The Doppler crystal directs its sound waves perpendicular to the myocardial wall, so changes in the fiber orientation across the wall should not affect the reflection of the sound pulse back to the probe. It has been shown that the myocardial fibers vary in orientation by about 110° from epicardium to endocardium [85]. In order for the ultrasonic crystals to correctly assess changes in segment length they need to be positioned along the same shortening axis [86]. Since the positions of the crystals can only be documented post-mortem, it is impossible to be confident of the crystal position during any given study.

Furthermore, when the ultrasonic technique is employed to measure transmural wall thickening, the crystal within the myocardial wall is subject to the rotational effects of contraction which may displace the orientation of the crystals and adversely affect signal quality. While the Doppler crystal signal may be affected by the same rotational effects, it is unlikely that the Doppler signal would be affected to the same degree [42] .

The third and most significant advantage of the Doppler crystal technique lies in its unique ability to sample thickening at various levels across the myocardial wall at the same location. The amplitude of the thickening signals obtained in this thesis were found to be proportional to the position of the range gated sample volume. This is in good agreement with previous reports using the same technique [45].

Transmural Thickening Relations

The transmural pattern of the calculated sub-transmural thickening fractions at baseline demonstrated a gradient favoring the endocardium, also in agreement with previous investigations [16, 44, 48-50]. The finding that the %TF in the Endo and Mw tended to equalize with dobutamine has not been

previously reported using the Doppler crystal technique. A related study by Gallagher using the transit time technique examined how the inner 1/2 and outer 1/2 (of the wall) %TF changed with exercise. The results of that study indicated that the gradient in thickening function remained constant with exercise, always favoring the endocardium [87]. The obvious difference between that study and this thesis is how the myocardial wall was divided for analysis. While the relationship between the Endo and Mw %TF was blurred during dobutamine in this study, the %TF for either of these was always greater than that in the Epi, supporting the constancy of the thickening gradient despite changes in myocardial performance.

Hemodynamic effects of graded dobutamine

In contrast to observations by other authors, we noted a much more dramatic response in the heart rate with graded dobutamine. Vatner reported that up to 40 ug/kg/min in a canine model that the heart rate increased 142% while we noted a 170% increase with a dose of only 15 ug/kg/min [88]. A potential explanation lies in the fact that pentobarbital anesthesia as employed by Vatner et al. has potent myocardial depressant properties [89]. Therefore, the heart rate response to dobutamine might have been blunted in comparison to that seen in this thesis where halothane anesthesia was employed.

The response of the systemic vasculature observed in this study is in full accord with the literature. Dobutamine is known to stimulate both α_1- and β_1- receptors in the vasculature [22]. These effects are felt to be relatively balanced resulting in little direct vascular effects. In this thesis, at the lower doses of dobutamine, mean AoP rose modestly (20%) then steadily declined as the level of dobutamine increased. The initial increase in systemic pressure was most likely related to the augmented inotropic state of the heart as evidenced by the early and pronounced increase in dP/dt (167% increase at D2.5 compared to baseline) and cardiac output (127% over baseline at D2.5) resulting in the higher systemic pressure. As the dose of dobutamine increased however, there was most likely a reflex withdrawal of sympathetic tone which resulted in a decrease in the vascular resistance (a 49% decline at D15.0 compared to baseline) and thus systemic arterial pressure.

Dobutamine effects on the coronary circulation

Dobutamine is also known to have effects on the canine coronary vasculature. We found a steady increase in Doppler epicardial LAD flow with graded dobutamine. This agrees with findings by other investigators that

epicardial coronary blood flow increases in parallel to demand with secondary coronary vasodilatation and decreased coronary resistance [90]. Dobutamine was shown in this thesis to have produced a marked increase in myocardial contractile performance and therefore demand, thus explaining the significant increases in observed flow.

At the sub-transmural level, we found that flow increased at all levels throughout graded dobutamine infusion with a gradient of flow favoring the epicardium in both perfusion territories. This gradient of flow is in contrast to that usually reported. Hoffman proposed after reviewing a number of experimental studies that the transmural gradient of flow was usually most altered in those models with an elaborate surgical preparation such as that used in this thesis [51]. The reasons for this are unclear, but may relate to changes in vagal tone and the use of halothane anesthesia. Vatner demonstrated that halothane (1%) had a tendency to dilate the epicardial coronary vasculature. This tendency was partially offset by the cardiac depressant effects of halothane which tended to produce a decrease in metabolic demand, and therefore constrict the coronary bed [91]. Since flow reserve is known to be less in the subendocardium than the subepicardium, the combined effects of halothane could operate to produce the gradient of flow favoring the epicardium observed in this study.

We noted in the post-dobutamine period that flow declined towards, but failed to return to, baseline values. While the half-life of intravenous dobutamine in humans is known to be about two minutes [22], no information is available regarding the half-life of the drug in dogs. It is therefore possible that the effects of dobutamine may persist beyond the time we expected and augmented flow and function 15 minutes (i.e. at the time of data collection) after maximal dobutamine had been terminated. Support for this theory could be taken from the fact that the heart rate, pressure-rate product, dP/dt, and cardiac output all behaved in a similar manner, failing to return to baseline after dobutamine was discontinued. It is also possible that the observations made here are an artifact of the small number of animals used for this study.

Study Limitations

Several potential sources of error may have adversely affected both data collection and analysis during the course of this project. The first and most important limitation of this thesis is the small number of experimental animals enrolled in the study. While pressure-thickening loop analysis has

been applied in more complex ischemic models in our laboratory, we chose a simpler, non-ischemic model to preliminarily define the role of the pressure-thickening loop as an index of changes in regional myocardial work.

As this model depended on the use of anesthetized animals, any inter-animal differences could have accounted for the variability observed in the hemodynamic, flow and thickening responses to dobutamine. In addition, the use of in vivo models is frequently complicated by the need to exclude experimental animals from analysis for various technical reasons. This study was no exception with only 70% (5 of 7) of the animals originally enrolled in the study being included in the final data set.

A limitation regarding the type of anesthesia used in this study lay in our inability to accurately measure the end-tidal concentration of halothane due to lack of equipment. This may have resulted in slightly different depths of anesthesia among the animals. While halothane is a known myocardial depressant, it has been shown that the most deleterious effects are not observed until an end-tidal concentration of 2% is reached [91]. The halothane concentration in this study was kept at an *inspired* concentration of 0.5-1.5%; if one assumes steady state conditions at the alveolar level, than it is unlikely that the halothane used in this study produced significant hemodynamic effects.

With reference to the collection of the thickening data, Zhu et al. examined how the position of the range gated sample volume with reference to the true end-diastolic depth affected the %TF measurement. They were able to show that errors of 1 mm in either direction did not produce appreciable artifacts when validated in the two-crystal setup described in the introduction of this thesis [44].

An additional source of error which could not be easily controlled for was the signal quality obtained with the Doppler crystal. Most of this error was observed with the crystal located in the LCX territory, as evidenced by the need to exclude this data from one of the animals used in this study. While at post-mortem analysis, no crystal was noted to be situated over a papillary muscle, it was occasionally found that the crystal was at or near the edge of one. Since the papillary muscle produces a tangential force on the endocardial surface during its function, crystals which sample thickening near the insertion point could have artifacts related to the papillary muscle

function. This was rarely an issue in the LAD territory due the more basal and lateral position of the papillary muscles relative to the anterior wall.

A methodologic limitation of the Doppler technique which was described earlier is the difficulty in quantifying the absolute left ventricular wall thickness. For the P-T loop analysis used here, this was not a problem since only the relative change in thickening (i.e. thickening excursion) was used to generate the loops. This inability to report true dimensions limits the application of real-world units of work to the area of the P-T loops. The loop area thus can only serve as a relative index of work, and not an absolute measure. The wall thickness could be estimated using the value of the range gate delay at which the blood pool was detected; however, this point would be difficult to consistently measure. This issue has recently been addressed with a new thickening module (Crystal Biotech, Holliston MA) which is able to reliably track the endocardial (or any other) point to give an accurate measure in millimeters of wall thickness.

Several lines of investigation have evaluated the gradient of pressure across the myocardial wall [95-98]. While not conclusive, most studies have shown that a pressure gradient exists favoring the endocardium. If true, concern regarding the assumption of constant transmural intra-myocardial pressure inherent to this thesis could be raised. No attempts to quantitate intra-myocardial pressure were made during the course of this study due to the difficult and unreliable technical methods currently available for this purpose. If, however, one assumes that the gradient of pressure exists, then corresponding reductions would need to be made in the measured P-T loop area to compensate for the reduced pressure at the Endo, Mw and Epi sub-regions compared to the LVP as measured with the Millar® catheter located within the left ventricular cavity.

A final methodologic limitation of this study is related to the determination of myocardial blood flow using the radiolabeled microsphere technique. Buckberg et al. summarized the potential errors associated with this technique and came to the conclusion that the error was minimized if (1) more than 400 microspheres were in each sample counted for flow (2) the microspheres were injected into the left atrium to ensure an even distribution in the bloodstream and (3) the microsphere technique was used in the dog. Since the microspheres are known to evenly distribute according to blood flow and at least 2 million microspheres were injected into the left atrium in this

canine model, then assuming that the heart receives 4% of its cardiac output we estimate that each of the 96 myocardial samples contained >400 microspheres, well above the level established by Buckberg for accuracy [92].

Future Applications

This preliminary validation of the use of the pressure-thickening loop as an index of sub-transmural work supports further testing of this approach in other animal models. As stated earlier, we have applied this approach in two other model systems as part of pilot studies. We first applied it in a canine model of myocardial stunning (n=2) produced by a 15 minute complete occlusion of the LAD with three hours of reperfusion. The use of the P-T loop in this setting showed promise as a means to track the temporal sequence of functional recovery and its modification with dobutamine. We also applied this technique in a model of critical coronary stenosis (n=2) with dobutamine stimulation in an effort to obtain a better understanding of the flow-function relationship in the presence of a non flow-limiting stenoses.

One aspect of the P-T loop which was not specifically addressed in this thesis was the change in loop morphology with dobutamine. We look forward to defining characteristic "loop responses" in shape as more data is collected on other animals since the limited number of animals in this study did not lend itself to this type of analysis. In addition, the P-T loop was not specifically analyzed with respect to the temporal sequence of contraction at the sub-transmural level. By superimposing temporally paired Endo, Mw and Epi loops on the same axes, it should be possible to examine the sequence of contraction across the myocardial wall. This analysis could also be applied to the raw thickening signal itself to obtain similar information.

While this thesis looked primarily at indices of systolic function and work, the pressure-thickening loop has the potential to provide useful information on diastolic function as well. The diastolic segment of the loop could easily be analyzed with respect to temporal parameters of diastolic thinning such as (1) the mean rate to one-half end-diastolic thinning and (2) the late-diastolic thinning fraction. These type of analyses could provide important information regarding diastolic dysfunction and its modification with inotropic agents.

Clinical Applications

A recent paper by Bolli et al. reported on the use of a modified Doppler thickening crystal on humans undergoing coronary artery bypass graft

surgery. This crystal was attached to a suction cup which was then positioned on the cardiac surface to measure the thickening fraction before and after surgery. This allowed the investigators to monitor functional recovery across the myocardial wall after revascularization [47]. The success of this application raises the possibility of generating P-T loops in the clinical setting during similar open chest procedures to monitor cardiac function and assess interventions aimed at maximizing function.

Summary

In this thesis, I have applied the use of a Doppler thickening crystal to generate sub-transmural left ventricular pressure-thickening loops which were first compared to independent indices of cardiac work and flow at the transmural level, then with flow at the level of the endocardium, midwall and epicardium with good results. The results of this analysis lend support to the use of these loops as a new index of regional work which provides information at a level of detail not available with other techniques. Future directions and potential clinical applications of this technique were outlined as well as the limitations of this approach. This type of approach will ultimately further the understanding of the complex interrelationship between myocardial flow, function and metabolism central to the management of patients with coronary artery disease and its complications.

TABLES 1-2

TABLE 1 Hemodynamics (All values +/- SEM)

	HR (n=5) (bpm)	Mean AoP (n=5) (mmHg)	Double Product (n=5) (mmHg x bpm)	Max dP/dt (n=3) (mmHg/sec)	Cardiac Output (n=3) (l/min)	SVR (n=3) (dyne/sec/cm 5)	Doppler Flow (n=3) (ml/min)(n=3)
Baseline	111.87 +/- 11.36	110.33 + - 7.41	14941 +/- 2151	1800 + - 329	2.45 +/- .29	3708 + - 242	31.5 + - 3.4
Dobutamine 2.5	116.18 +/- 13.39	126.36 + - 5.79	17900 +/- 2071	2820 + - 460	2.95 + - .28	3393 + - 394	37.6 +/- 3.6
Dobutamine 5.0	126.50 + - 13.96	125.40 + - 4.61	19967 +/- 1937	3279 +/- 582	3.36 +/- .04	2850 +/- 140	43.9 +/- 9.5
Dobutamine 7.5	146.70 +/- 11.33	116.60 + - 3.93	21646 +/- 1089	4398 + - 717	3.60 + - .34	2597 +/- 328	48.0 + - 10.8
Dobutamine 10.0	162.90 + - 7.58	115.70 + - 3.53	23572 +/- 848	5089 + - 864	3.86 +/- .46	2421 + - 308	59.3 +/- 12.4
Dobutamine 15.0	180.17 +/- 8.75	112.33 + - 2.84	25377 +/- 1032	4614 + - 731	4.51 +/- .55	1989 + - 281	74.2 +/- 7.1
Post Dobutamine	128.00 + - 9.04	103.43 + - 4.83	16294 +/- 1043	2506 + - 746	2.84 + - .12	2795 + - 174	46.5 +/- 8.9

TABLE 2 Microsphere Flow (ml/min/gm +/- SEM) (N=3)

	LAD				LCX			
	Endocardium	Midwall	Epicardium	Transmural	Endocardium	Midwall	Epicardium	Transmural
Baseline	1.01 + - 0.13	1.01 +/- 0.14	1.21 +/- 0.15	1.08 +/- 0.14	1.13 + - 0.15	1.06 + - 0.15	1.10 +/- 0.18	1.10 + - 0.16
Dobutamine 5.0	1.21 + - 0.31	1.34 +/- 0.30	1.58 + - 0.32	1.38 +/- 0.30	1.38 +/- 0.30	1.41 + - 0.36	1.46 +/- 0.39	1.42 +/- 0.36
Dobutamine 10.0	1.38 + - 0.43	1.59 + - 0.42	1.86 + - 0.45	1.61 +/- 0.43	1.67 + - 0.52	1.80 + - 0.65	1.77 + - 0.57	1.75 + - 0.58
Dobutamine 15.0	1.77 + - 0.47	2.01 + - 0.46	2.37 + - 0.49	2.05 +/- 0.47	2.08 + - 0.60	2.32 + - 0.78	2.26 +/- 0.62	2.22 + - 0.67
Post Dobutamine	1.31 + - 0.30	1.36 + - 0.33	1.47 + - 0.30	1.38 +/- 0.31	1.47 +/- 0.37	1.47 +/- 0.40	1.34 + - 0.34	1.43 + - 0.37

TABLES 3-4

TABLE 3 PERCENT THICKENING FRACTION DATA (%TF) (N=3)

	LAD				LCX			
	Endocardium	Midwall	Epicardium	Transmural	Endocardium	Midwall	Epicardium	Transmural
Baseline	14.93 +- 8.58	19.49 +/- 4.50	6.83 +/- 1.17	13.30 +/- 4.54	23.69 +/- 4.86	16.61 +/- 0.18	5.95 +/- 0.02	15.53 +/- 1.68
Dobutamine 2.5	24.52 +/- 7.88	29.46 +/- 5.88	11.41 +/- 2.38	21.46 +/- 5.15	26.88 +/- 1.55	20.34 +/- 1.57	9.26 +/- 1.69	18.77 +/- 1.63
Dobutamine 5.0	30.49 +- 5.95	28.15 +/- 5.22	14.51 +/- 2.08	23.96 +/- 3.86	19.56 +/- 4.07	21.50 +/- 0.89	10.41 +/- 1.15	17.12 +/- 2.05
Dobutamine 7.5	36.51 +/- 4.68	29.98 +/- 4.77	14.84 +/- 2.26	26.45 +/- 2.96	25.99 +/- 4.04	21.20 +/- 2.19	11.11 +/- 0.59	19.40 +/- 2.26
Dobutamine 10.0	36.89 +/- 0.80	32.75 +/- 3.55	13.77 +/- 1.31	27.36 +/- 2.00	24.17 +/- 3.48	19.08 +/- 1.59	13.42 +/- 1.45	18.99 +/- 2.13
Dobutamine 15.0	33.67 +- 0.48	34.29 +/- 2.86	16.54 +/- 2.76	27.66 +/- 1.77	27.85 +/- 4.85	19.63 +/- 3.01	11.99 +/- 0.76	19.78 +/- 2.76
Post Dobutamine	19.20 +- 5.91	16.27 +/- 2.59	9.63 +/- 0.97	14.14 +/- 3.15	15.96 +/- 2.81	17.19 +/- 1.62	6.6 +/- 0.84	13.19 +/- 1.78

TABLE 4 PRESSURE THICKENING LOOP AREAS (sq. pixels) (N=3)

	LAD				LCX			
	Endocardium	Midwall	Epicardium	Transmural	Endocardium	Midwall	Epicardium	Transmural
Baseline	3417 + - 1247	5294 +/- 1053	1993 +/- 251	10704 +/- 53	6036 +/- 599	4493 +/- 219	1804 +- 43	12333 +/- 776
Dobutamine 2.5	7409 + - 1118	8495 +/- 685	3452 +/- 356	17356 +/- 909	9343 +/- 1669	6839 +/- 60	2904 + - 992	19086 +/- 617
Dobutamine 5.0	8671 +/- 1402	5949 +/- 1038	4125 +/- 136	18745 +/- 1176	6694 +/- 237	7439 +/- 243	3464 +/- 730	17595 +/- 735
Dobutamine 7.5	10294 +/- 217	6628 +/- 949	3941 +/- 934	20864 +/- 1426	6968 +/- 540	7073 + - 1420	3570 +/- 403	17611 +/- 2362
Dobutamine 10.0	11002 +- 718	7053 +/- 668	3214 +/- 112	21269 +/- 1079	8093 + - 2478	6410 +/- 140	4104 +/- 674	18606 +/- 3012
Dobutamine 15.0	11408 +/- 1102	6582 +/- 884	4095 +/- 583	22085 +/- 1473	8618 + - 1129	5259 +/- 1238	3910 + - 39	17787 +/- 2328
Post Dobutamine	5066 + - 1368	4868 +/- 962	3315 +/- 1002	13248 +/- 3266	4865 +/- 1474	4798 +/- 2187	1837 +/- 1253	11501 +/- 4915

Table 5 Correlative Data Analysis

First Variable	Second Variable	df (n-2)	r	r squared	Sigificance
Trasmural					
LAD Loop Area	Regional MVO2	13	0.524	0.274	p < .05
LAD Loop Area	dP/dt	13	0.814	0.663	p < .01
LAD Loop Area	P-R Product	13	0.648	0.420	p < .01
LAD Loop Area	LAD Tm uSphere Flow	13	0.633	0.401	p < .05
LCX Loop Area	dP/dt	8	0.822	0.676	p < .01
LCX Loop Area	P-R Product	8	0.917	0.841	p < .01
LCX Loop Area	LCX Tm uSphere Flow	8	0.879	0.773	p < .01
LAD uSphere Flow	Regional MVO2	13	0.886	0.785	p < .01
LAD uSphere Flow	dP/dt	13	0.863	0.744	p < .01
LAD uSphere Flow	P-R Product	13	0.912	0.831	p < .01
LCX uSphere Flow	dP/dt	8	0.871	0.758	p < .01
LCX uSphere Flow	P-R Product	8	0.901	0.811	p < .01
Endocardium					
LAD uSphere Flow	LAD Loop Area	13	0.256	0.056	NS
LCX uSphere Flow	LCX Loop Area	8	0.917	0.841	p < .01
Midwall					
LAD uSphere Flow	LAD Loop Area	13	0.572	0.328	p < .05
LCX uSphere Flow	LCX Loop Area	8	0.523	0.273	NS
Epicardium					
LAD uSphere Flow	LAD Loop Area	13	0.681	0.463	p < .01
LCX uSphere Flow	LCX Loop Area	8	0.766	0.587	p < .01

Figure 1

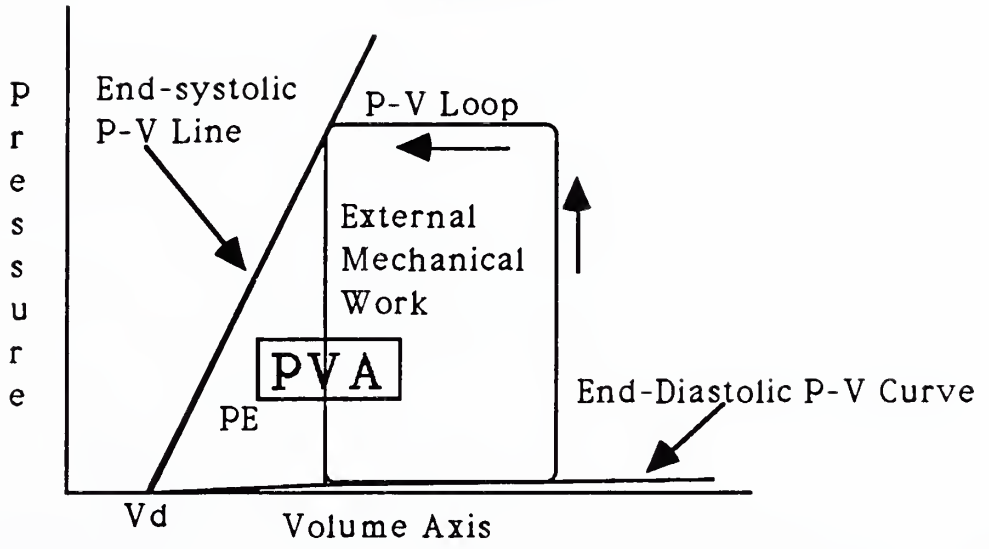

Figure 1: Schematic drawing of the P-V diagram of the left ventricle. P-V loop is the tragectory of an ejecting contraction. The systolic segment (heavy curve) of the trajectory starts at a point on the end-diastolic P-V relation curve and ends at a point on the end-systolic P-V relation line. The rectangular area under the systolic segment of the P-V trajectory is equivalent to the external mechanical work of the contraction. The triangular area under the end-systolic P-V line between its volume intercept (Vd) and the end-systolic P-V point is equivalent to the end-systolic potential energy. The sum of these two areas is the pressure-volume area (PVA).

Figure 2

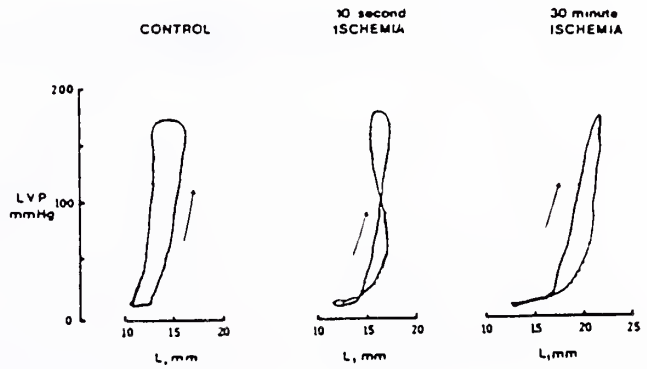

Figure 2: Instantaneous X-Y plots of left ventricular pressure vs. segmental length (mm) as measured with a segment length gauge. From left to right are pressure-length (P-L) loops under control, 10 seconds of ischemia and 30 min of ischemia. (Adapted from Tyberg, 1974).

Figure 3

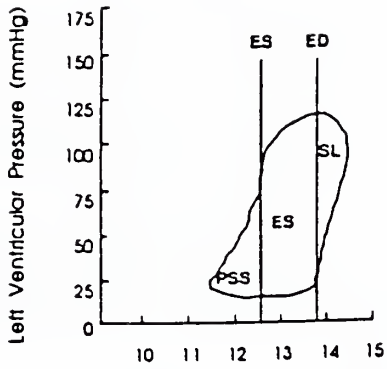

Figure 3: Pressure-length loop obtained from the LAD territory during mild ischemia. End-diastole (ED), defined by the initial upstroke of the first derivative of left ventricular pressure (dP/dt), and end-systole(ES) defined by the return of aortic flow to zero are indicated by vertical lines. ES = effective shortening area; PSS = post systolic shortening area; SL = systolic lengthening area (adapted from Safwat, 1991).

Figure 4

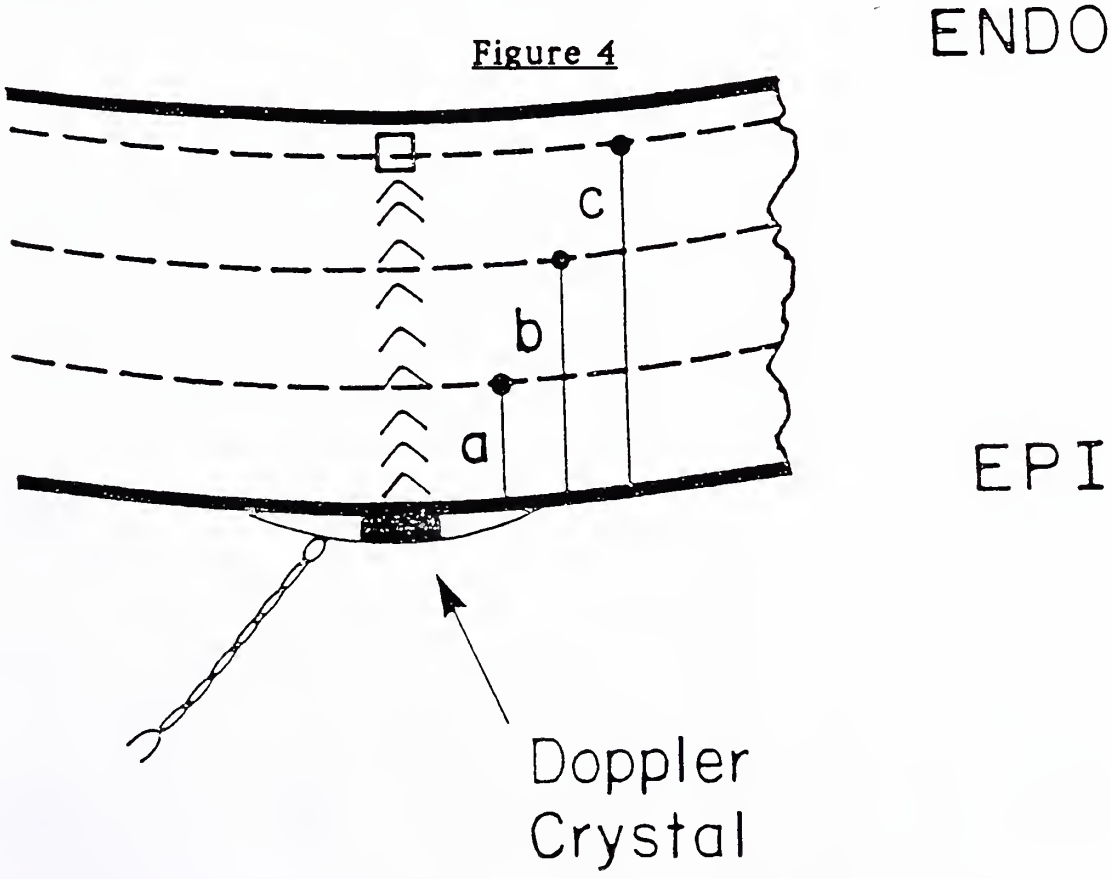

Figure 4: This schematic cut-away of a portion of the myocardial wall demonstrates the use of the epicardial Doppler crystal to measure thickening across the wall. The sample volume () is shown at three positions across the wall, corresponding to outer 1/3 (a), outer 2/3 (b) and transmural (i.e. full thickness) (c) thickening (reproduced with permission from Edwards, 1991).

Figure 5

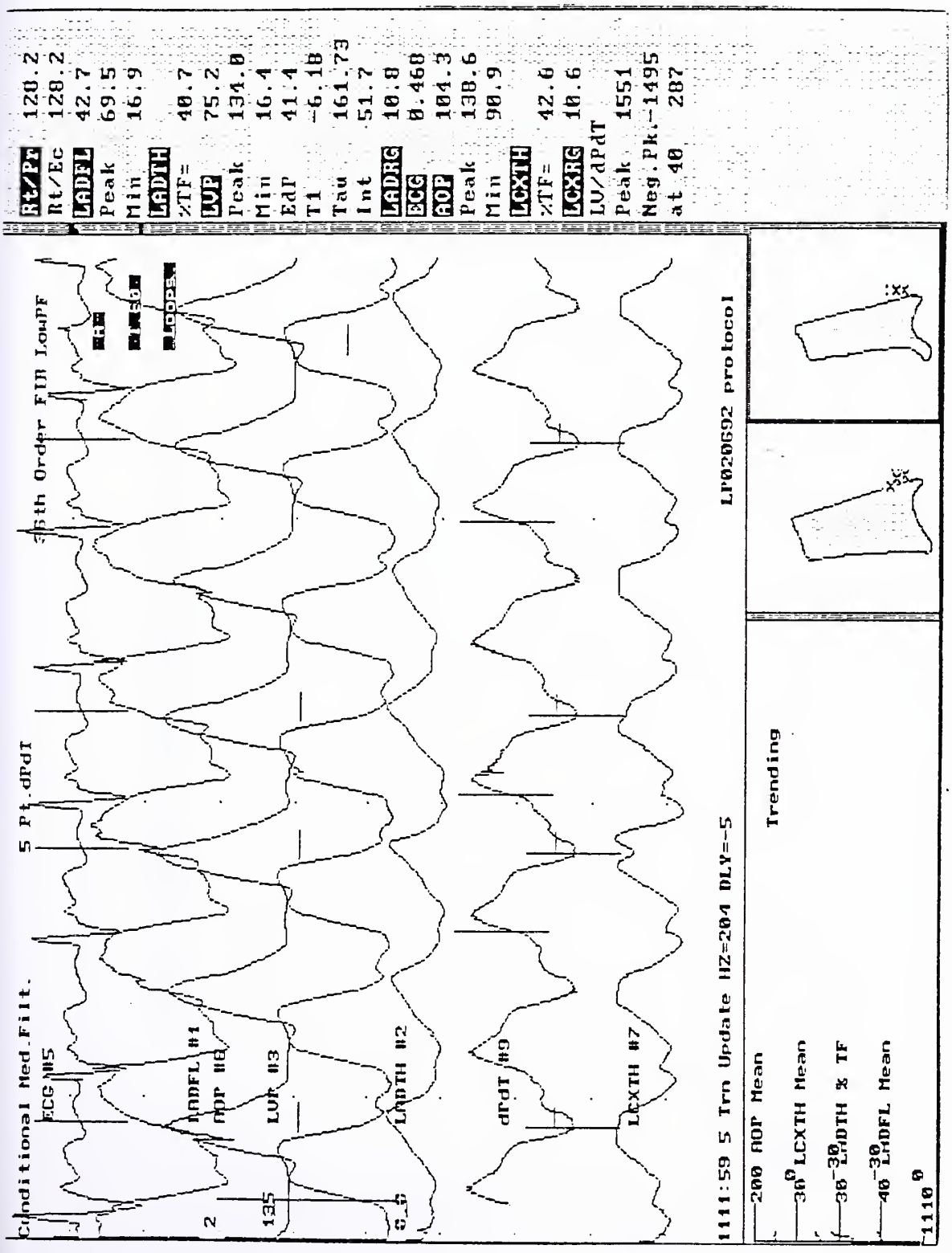

Figure 5: Shown here is a typical screen display from the DATAFLOW® program showing the waveform display at center; the various computed statistics for each channel at right; the trending file in the lower left; and real-time pressure-thickening loops for both the LAD (left) and LCX (right) in the lower right corner.

Figure 6

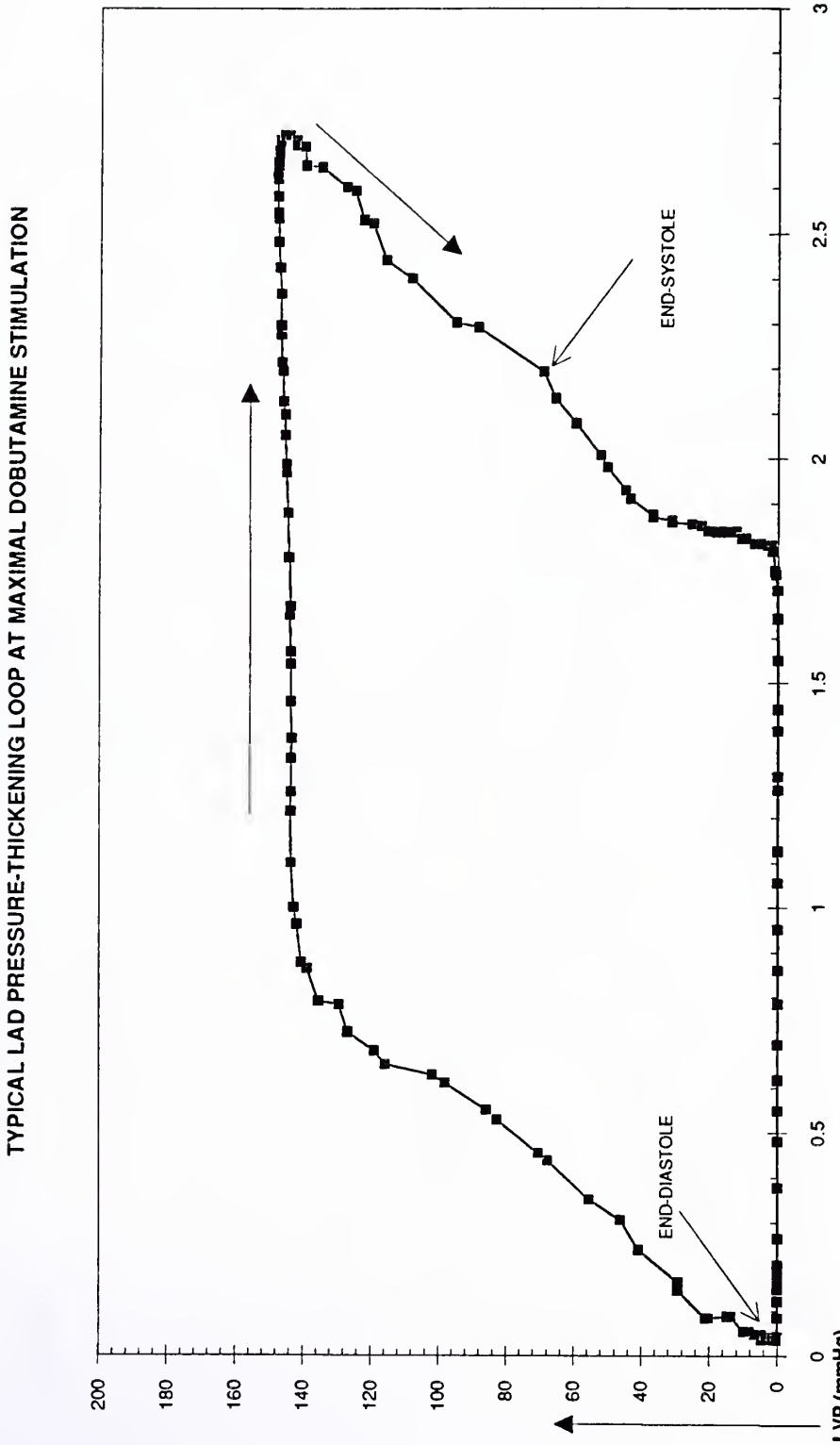

Figure 6: Shown in this figure is a typical transmural pressure-thickening loop from the LAD territory during maximal dobutamine (15.0 ug/kg/min) stimulation. The single loop here represents the average of five (5) cardiac cycles obtained during one of the DATAFLOW® manual saves. Left ventricular pressure (mmHg) is plotted on the Y-axis and thickening (mm) is plotted on the x-axis. The end-diastolic and end-systolic points are labeled as is the clockwise rotation of the loop.

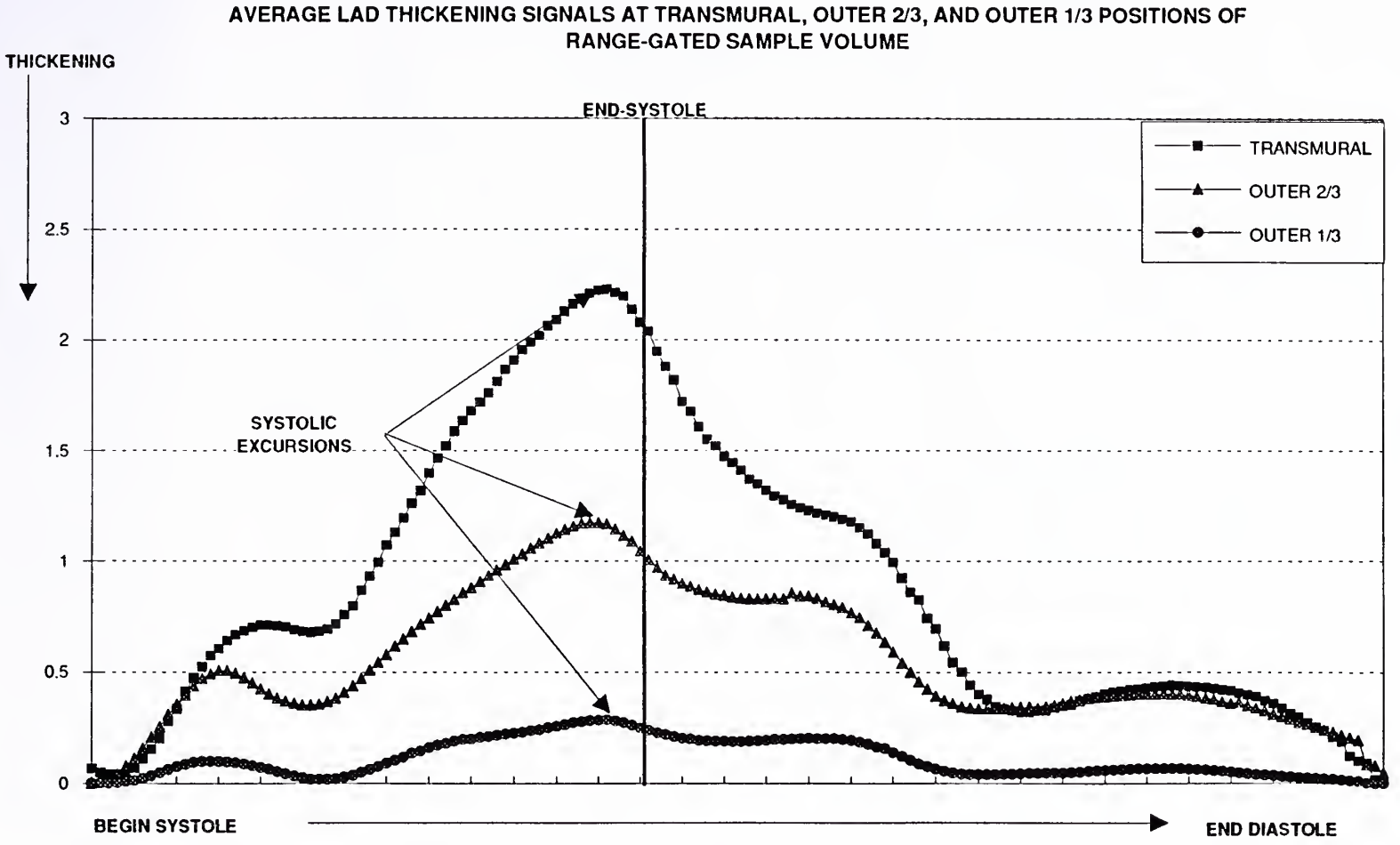

Figure 7

Figure 7: This figure depicts the average thickening signal from the LAD territory during baseline for the (1) transmural (2) outer 2/3 and (3) outer 1/3 positions of the range-gated sample volume. Each thickening signal is the average of five full cardiac cycles. Shown in the figure is the end-systolic time point based on the peak negative value of dP/dt. Also shown are the respective maximal systolic excursions which are used in the thickening fraction equation as described under Materials and Methods. To note is the gradient of the thickening signal (and therefore maximal systolic excursion) which favors the deeper myocardial layers.

Figure 8 (a-c)

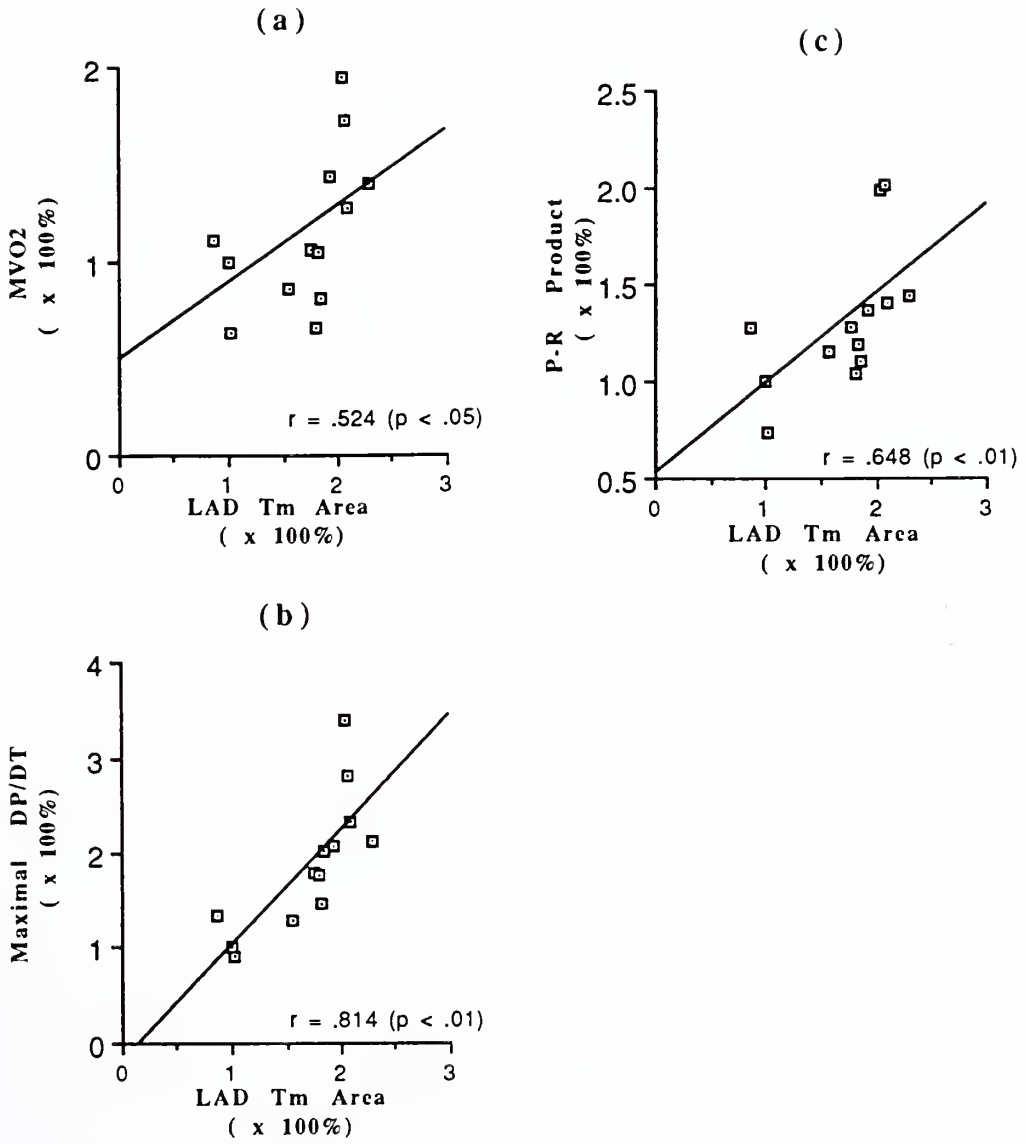

Figure 8 (a-c): Shown here are the scatter plots with their respective correlations and significance levels for the LAD Transmural P-T loop area (LAD Tm Area) vs. the MVO_2 (a), maximal dP/dt (b), and P-R product (c). All data points are expressed as % change from baseline in order to facilitate incorporation of multiple animals into the data set. Of particular note are the good correlations observed between the Tm P-T loop area and the other variables.

Figure 9 (a-b)

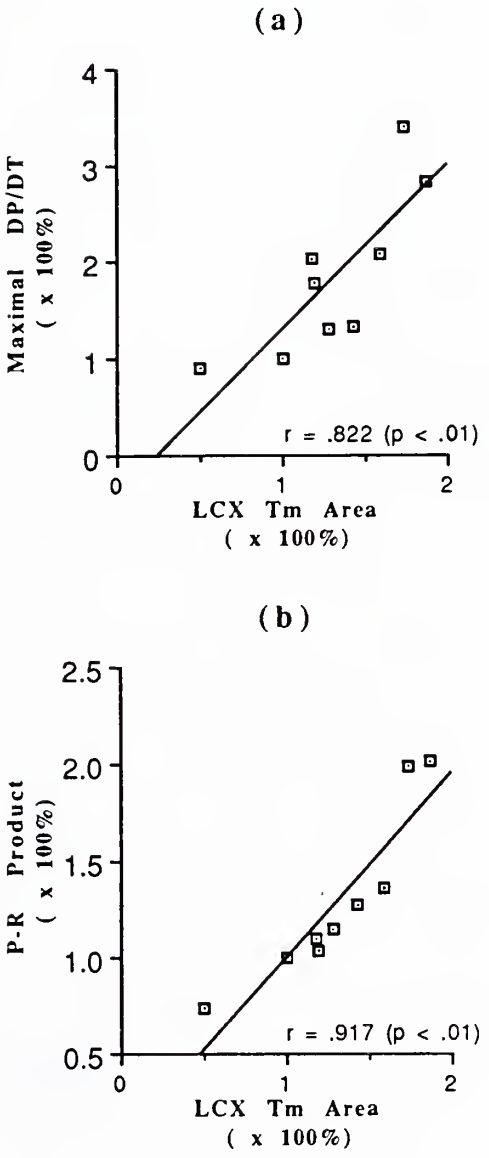

Figure 9 (a-b): In this figure are shown the scatter plots with their respective correlations and significance levels for the LCX transmural P-T loop area (LCX Tm area) vs. the maximal dP/dt (a) and P-R product (b). All data points are expressed as % change from baseline in order to facilitate incorporation of multiple animals into the data set. Again, good correlations were noted between the Tm loop area and hemodynamic indices of myocardial work.

Figure 10 (a-d)

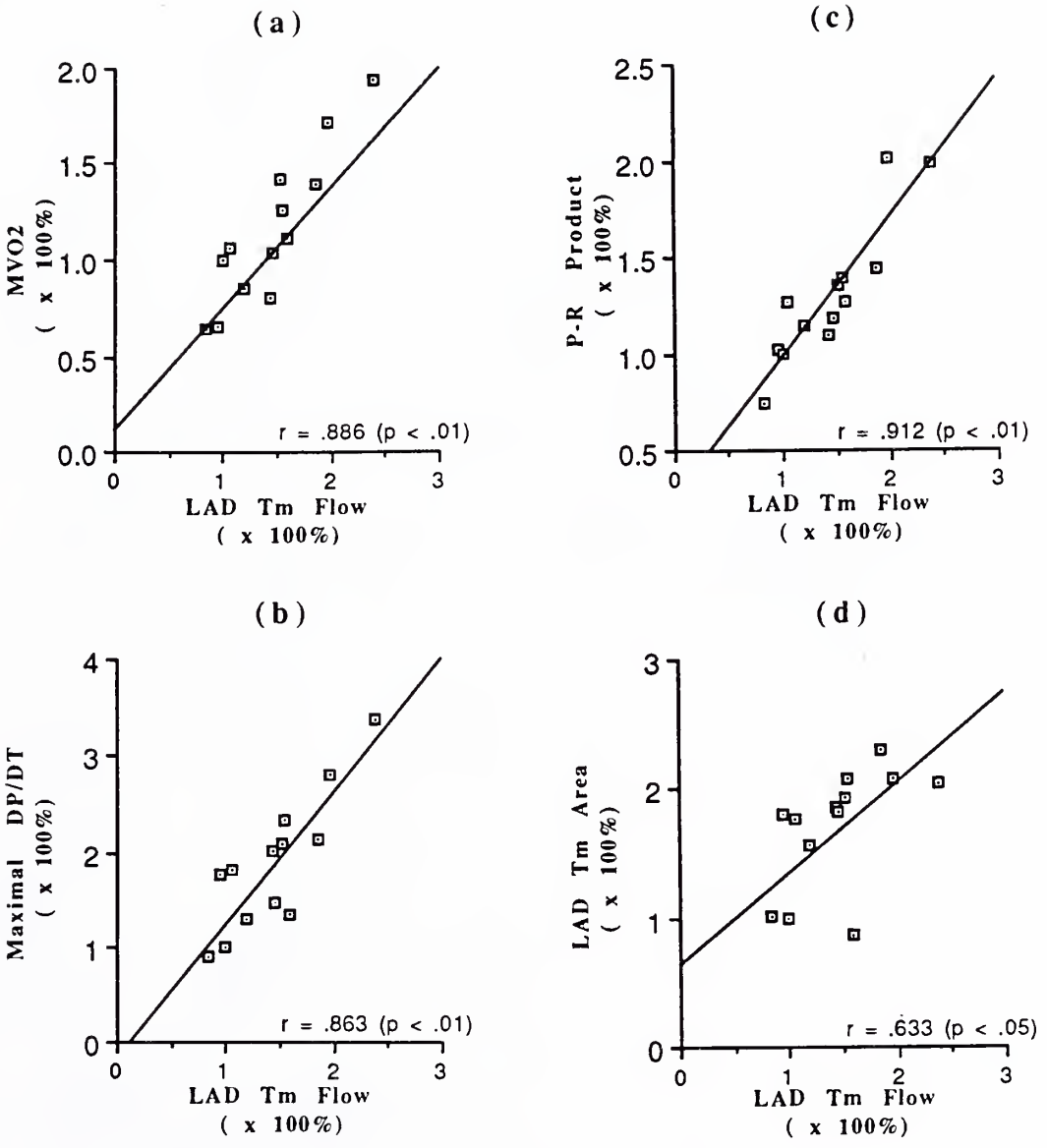

Figure 10 (a-d): In this figure, the scatter plots for the LAD transmural microsphere flow (LAD Tm flow) vs. the MVO_2 (a), maximal dP/dt (b), P-R product (c), and Tm P-T loop area (LAD Tm Area) (d) are shown; again with their respective correlations and significance levels. All data points are expressed as % change from baseline in order to facilitate incorporation of multiple animals into the data set. As seen above, flow at the transmural level significantly correlated with both metabolic (MVO_2) and hemodynamic (maximal dP/dt and P-R product) indices of myocardial work in addition to the P-T loop area. Flow thus appears to function as an indirect marker of work in this animal preparation.

Figure 11 (a-c)

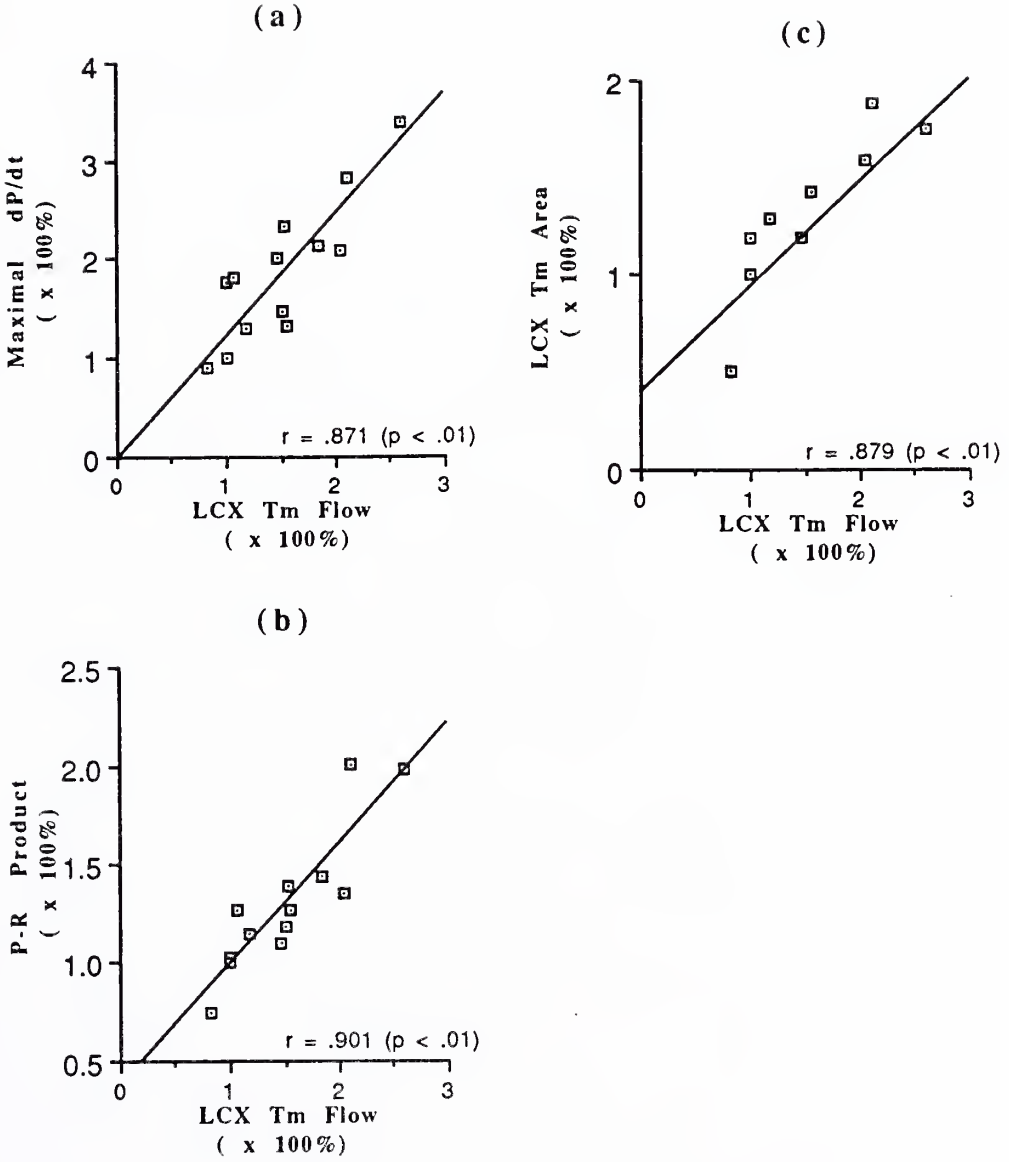

Figure 11 (a-c): Similar to Figure 10 above, this figure depicts the scatter plots for the LCX transmural microsphere flow (LCX Tm flow) vs. the maximal dP/dt (a), P-R product (b) and Tm P-T loop area (c). Once again, significant correlations were found in all cases. As the MVO_2 was only measured in the LAD territory, this metabolic index of work was not used for comparison to the LCX Tm flow. All data points are expressed as % change from baseline in order to facilitate incorporation of multiple animals into the data set.

Figure 12 (a-c)

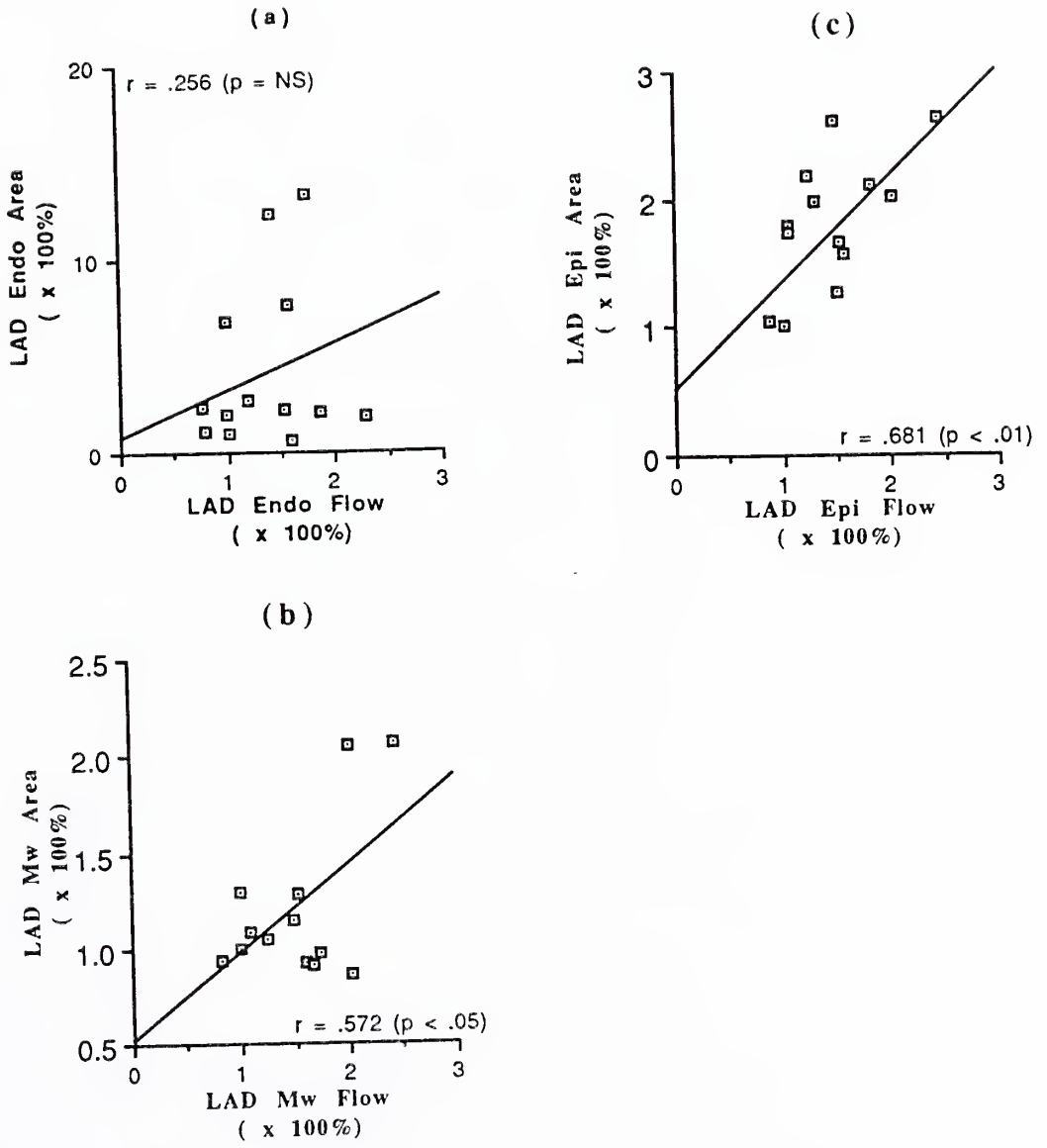

Figure 12 (a-c): In this figure, the respective sub-transmural (i.e. endocardial (a), midwall (b), and epicardial (c)) microsphere flows and P-T loop areas are compared for the LAD territory. While positive correlations were noted in all cases, statistical significance was only achieved for the midwall and epicardial sub-regions. All data points are expressed as % change from baseline in order to facilitate incorporation of multiple animals into the data set.

Figure 13 (a-c)

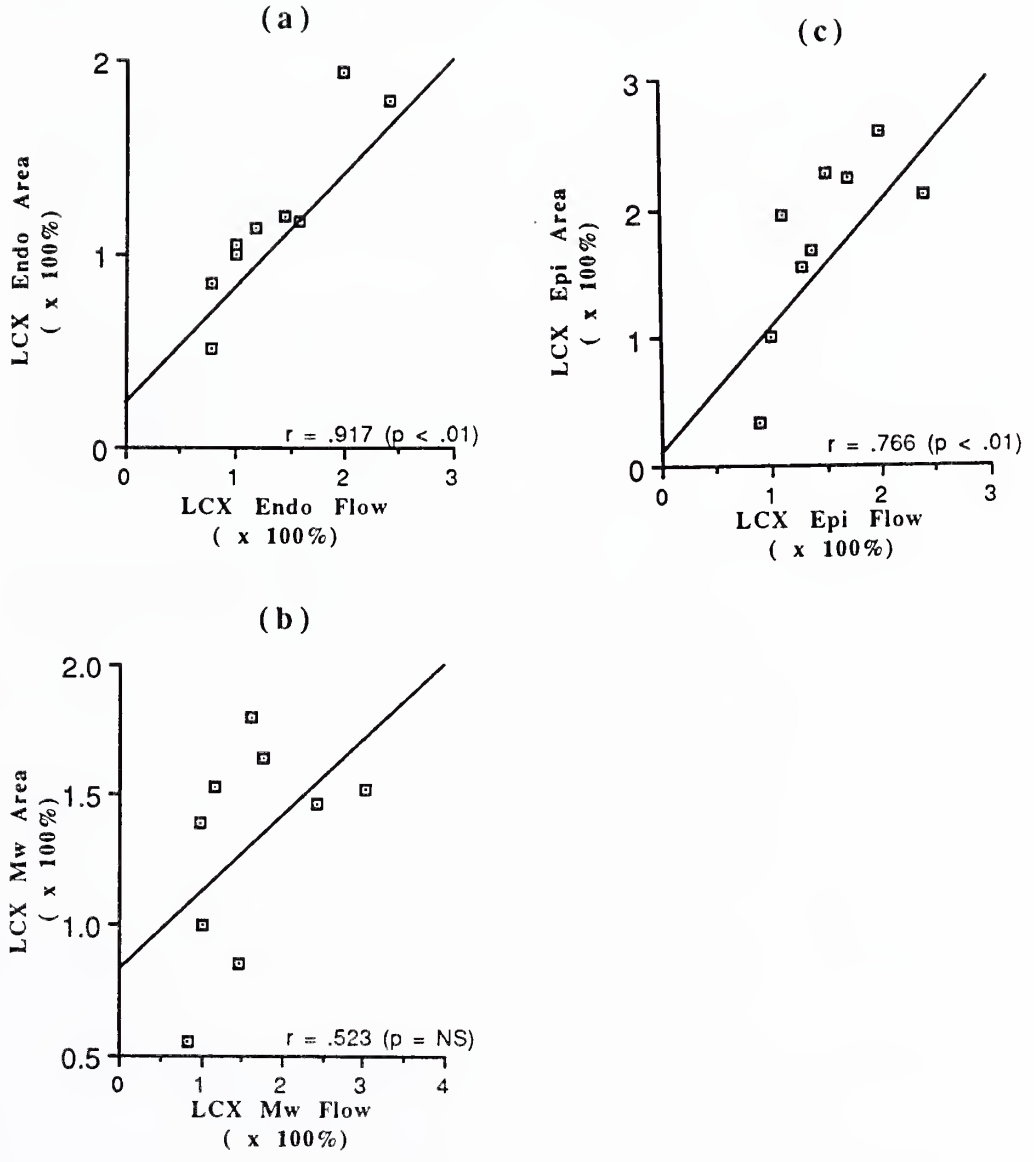

Figure 13 (a-c): In this figure, the respective LCX territory sub-transmural (i.e. endocardial (a), midwall (b), and epicardial (c)) microsphere flows and P-T loop areas are compared. While positive correlations were again noted in all cases, in this case statistical significance was only achieved for the endocardial and epicardial sub-regions. All data points are expressed as % change from baseline in order to facilitate incorporation of multiple animals into the data set.

Acknowledgments

- I wish to thank Dr. Albert J. Sinusas for your role as mentor and thesis advisor. Your critical insight and attention to detail proved invaluable in the development and completion of this thesis project. I am grateful for the opportunity you have given me to develop my academic ideals. I look forward to other profitable collaborations as time goes on.

- I would like to thank Dr. Larry Young for your support and utter flexibility in keeping up with ever our changing experimental plans during the course of this project. Your advice and perspective have helped to shape my views of the field of cardiology as well as its inner workings.

- I would like to give a special thanks to Dr. Barry Zaret whose ability to see the "big" picture helped to focus this project into a definable entity. I sincerely appreciate your time, advice and understanding you have shown me as my academic advisor during the past two years. I hope to continue this relationship as I proceed to make increasingly important decisions about my future as a budding cardiologist.

- I would also like to thank Qing Xin Shi and Jonathon Alderman whose technical support were invaluable for this project.

Bibliography

1. Braunwald, E. and R.A. Kloner, *The stunned myocardium: Prolonged, postischemic ventricular dysfunction.* Circulation, 1982. **66**(6): p. 1146-1149.

2. Braunwald, E. and J.D. Rutherford, *Reversible ischemic left ventricular dysfunction: Evidence for the "hibernating myocardium".* Journal of the American College of Cardiology, 1986. **8**(6): p. 1467-70.

3. Kloner, R.A., K. Przyklenk, and B. Patel, *Altered myocardial states.* The American Journal of Medicine, 1989. **86**(suppl 1a): p. 14-22.

4. Marban, E., *Myocardial stunning and hibernation.* Circulation, 1991. **83**(2): p. 681-688.

5. Reduto, L.A.*et.al.*, *Coronary artery reperfusion in acute myocardial infarction: beneficial effects of intra-coronary streptokinase on left ventricular salvage and performance.* American Heart Journal, 1981. **102**: p. 1168-1177.

6. Stack, R.S.*et.al.*, *Functional improvement of jeopardized myocardium following intracoronary streptokinase infusion in acute myocardial infarction.* Journal of Clinical Investigation, 1983. **72**: p. 84-95.

7. Anderson, J.L., H.W. Marshall, and B.E. Bray, *A randomized trial of intracoronary streptokinase in the treatment of acute myocardial infarction.* New England Journal of Medicine, 1983. **308**: p. 1313-1318.

8. Wijns, W.*et.al.*, *Effect of coronary occlusion during percutaneous transluminal coronary angioplasty in humans on left ventricular chamber stiffness and regional diastolic pressure-radius relations.* Journal of the American College of Cardiology, 1986. **7**: p. 455-463.

9. Heyndrickx, G.R., *et al.*, *Depression of regional blood flow and wall thickening after brief coronary occlusions.* American Journal of Physiology, 1978. **234**: p. H653.

10. Rahimtoola, S.H., *A perspective on the three large multicenter randomized clinical trials of coronary bypass surgery for chronic stable angina.* Circulation, 1985. **72(suppl V)**: p. V123-V135.

11. Bristow, J.D., *et al.*, *Response to myocardial ischemia as a regulated process.* Circulation, 1991. **84**(6): p. 2580-2587.

12. Ross, J.J., *Myocardial perfusion-contraction matching.* Circulation, 1991. **83**(3): p. 1076-1083.

13. Shearn, D.L. and B. B.N., *Coronary artery bypass surgery in patients with left ventricular dysfunction.* American Journal of Medicine, 1986. **80**: p. 405-411.

14. Nesto, R.W.*et.al.*, *Inotropic contractile reserve: A useful predictor of increased 5 year survival and improved postoperative left ventricular function in patients with coronary artery disease and reduced ejection fraction.* The American Journal of Cardiology, 1982. **50**(July): p. 39-44.

15. Matsuzaki, M., *et al.*, *Sustained regional dysfunction, produced by prolonged coronary stenosis: Gradual recovery after reperfusion.* Circulation, 1983. **68**: p. 170-182.

16. Edwards, N.C., *et al.*, *Influence of subendocardial ischemia on transmural myocardial function.* American Journal of Physiology, 1992. **(in press)**.

17. Liedtke, J.A., *et al.*, *Changes in substrate metabolism and effects of excess fatty acids in reperfused myocardium.* Circulation Research, 1988. **62**: p. 535-542.

18. Feigenbaum, H., *Echocardiography.* Fourth ed. 1986, New York: Lea & Febiger.

19. Mendoza, C.A., M.H. Crawford, and R.A. O'Rourke, *Evaluating left ventricular function.*, in *The practice of echocardiography.*, R. Kraus, Editor. 1985, John Wiley & Sons: New York. p. 273-292.

20. Zoghbi, W.A., *et al.*, *End-systolic radius to thickness ratio: An echocardiographic index of regional performance during reversible myocardial ischemia in the conscious dog.* Journal of the American College of Cardiology, 1987. **10**(5): p. 1113-1121.

21. Higgins, C.B., *New cardiac imaging techniques.*, in *Harrison's Principles of Internal Medicine*, J.D. Wilson, *et al.*, Editor. 1991, McGraw-Hill, Inc.: New York. p. 865-871.

22. Lawless, C.E. and H.S. Loeb, *Pharmacokinetics and pharmacodynamics of dobutamine*, in *Dobutamine*, K. Chatterjee, Editor. 1989, NCM Publishers, Inc.: New York. p. 33-48.

23. Bendersky, R., *et al.*, *Dobutamine in chronic ischemic heart failure: Alterations in left ventricular function and coronary hemodynamics.* The American Heart Journal, 1981. **48**(September 1981): p. 554-8.

24. Horn, H.R.*et.al.*, *Augmentation of left ventricular contraction pattern in coronary artery disease by an inotropic catecholamine: The epinephrine ventriculogram.* Circulation, 1974. **49**(June): p. 1063-1071.

25. Vatner, S.F., *et al.*, *Effects of catecholamines, exercise and nitroglycerin on the normal and ischemic myocardium in conscious dogs.* Journal of Clinical Investigation, 1974. **54**: p. 563-575.

26. Bolli, R., *et al.*, *Beta-adrenergic stimulation reverses postischemic myocardial dysfunction without producing subsequent functional deterioration,*. The American Journal of Cardiology, 1985. **56**(December 1): p. 964-968.

27. Arnold, J.M.O., *et al., Inotropic Stimulation or reperfused myocardium with dobutamine: Effects on infarct size and myocardial function.* The American Journal of Cardiology, 1985. **6**(November): p. 1026-34.

28. Ellis, S.G.*et.al., Response of reperfusion-salvaged, stunned myocardium to inotropic stimulation.* American Heart Journal, 1984. **107**(January): p. 13-19.

29. Maroko, P.R., P. Libby, and E. Braunwald, *Effect of pharmacologic agents on the function of the ischemic heart.* The American Journal of Cardiology, 1973. **32**: p. 930-936.

30. Vatner, S.F. and H. Baig, *Importance of heart rate in determining the effects of sympathomimetic amines on regional myocardial function and blood flow in conscious dogs with acute myocardial ischemia.* Circulation Research, 1979. **45 No.6**(December): p. 793-803.

31. Tuttle, R.R. and J. Mills, *Dobutamine: Development of a new catecholamine to selectively increase contractility.* Circulation Research, 1975. **36**: p. 185-196.

32. Gillespie, T.A.*et.al., Effects of Dobutamine in Patients with Acute Myocardial Infarction.* The American Journal of Cardiology, 1977. **39**(April 1977): p. 588-594.

33. Goldstein, R.A., *Dobutamine in acute myocardial infarction,* in *Dobutamine*, K. Chatterjee, Editor. 1989, NCM Publishers, Inc.: New York. p. 83-96.

34. Francis, G.S., *Dobutamine in chronic congestive heart failure.,* in *Dobutamine*, K. Chatterjee, Editor. 1989, NCM Publishers, Inc.: New York. p. 97-108.

35. Chatterjee, K., *Summary of clinical applications and practical considerations of dobutamine therapy.,* in *Dobutamine*, K. Chatterjee, Editor. 1989, NCM Publishers, Inc.: New York. p. 173-174.

36. Mason, J.R.*et.al., Thallium scintigraphy during dobutamine infusion: Nonexercise-dependent screening test for coronary disease.* American Heart Journal, 1984. **107**(March 1984): p. 481-485.

37. Konishi, T.*et.al., Radionuclide assessment of left ventricular function during dobutamine infusion in patients with coronary artery disease: Comparison with ergometer exercise.* Clinical Cardiology, 1989. **13**(March): p. 183-188.

38. Piérard, L.A.*et.al., Identification of viable myocardium by echocardiography during dobutamine infusion in patients with myocardial infarction after thrombolytic therapy: Comparison with positron emission tomography.* Journal of the American College of Cardiology, 1990. **15, No. 5**(April): p. 1021-31.

39. Liang, C.-S.*et.al., Dobutamine infusion in conscious dogs with and without acute myocardial infarction.* Circulation Research, 1981. **49**(July): p. 170-180.

40. Berrizbeitia, L.D.*et.al.*, *Inotropic response of the salvaged myocardium after acute coronary occlusion.* The Annals of Thoracic Surgery, 1986. **41** No. 1(January): p. 58-64.

41. Schulz, R.*et.al.*, *Consequences of regional inotropic stimulation of ischemic myocardium on regional myocardial blood flow and function in anesthetized swine.* Circulation Research, 1988. **64**(June): p. 1116-1126.

42. Hartley, C.J.*et.al.*, *Doppler measurement of myocardial thickening with a single epicardial transducer.* American Journal of Physiology, 1983. **245**: p. H1066-H1072.

43. Hartley, C.J., *et al.*, *Synchronized pulsed Doppler blood flow and ultrasonic dimension measurements in conscious dogs.* Ultrasound in Medicine and Biology, 1978. **4**: p. 99-110.

44. Zhu, W.-X., *et al.*, *Validation of a single crystal for measurement of transmural and epicardial thickening.* American Journal of Physiology, 1986. **251**: p. H1045-H1055.

45. Bolli, R., *et al.*, *Nonuniform transmural recovery of contractile function in stunned myocardium.* American Journal of Physiology, 1989. **257**: p. H375-H385.

46. Charlat, M.L., *et al.*, *Prolonged abnormalities of left ventricular diastolic wall thinning in the "stunned" myocardium in conscious dogs: Time course and relation to systolic function.* Journal of the American College of Cardiology, 1989. **13**(1): p. 185-194.

47. Bolli, R. and C.J. Hartley, *An accurate, nontraumatic ultrasonic method to monitor myocardial wall thickening in patients undergoing cardiac surgery.* Journal of the American College of Cardiology, 1990. **15**(5): p. 1055-1065.

48. Sabbah, H.N., M. Marzilli, and P.D. Stein, *The relative role of subendocardium and subepicardium in left ventricular mechanics.* American Journal of Physiology, 1981. **240**: p. H920-H926.

49. Gallagher, K.P.*et.al.*, *Dissociation between epicardial and transmural function during acute myocardial ischemia.* Circulation, 1985. **71**(6): p. 1279-1291.

50. Hattori, S., *et al.*, *Contrasting ischemic contraction patterns by zone and layer in canine myocardium.* American Journal of Physiology, 1982. **243**: p. H852-H855.

51. Hoffman, J., *Transmural Myocardial Perfusion.* Progress in Cardiovascular Diseases, 1987. **29**(6): p. 429-464.

52. Rudolph, A.M. and M.A. Heymann, *The circulation of the fetus in utero. Methods for studying distribution of blood flow, cardiac output and organ blood flow.* Circulation Research, 1967. **21**: p. 163-184.

53. Reneman, R.S. and A. Verheyen. *The radioactive microsphere method.* in *9th European Conference on Microcirculation.* 1976. Antwerp:

54. Heymann, M.A., *et al., Blood flow measurements with radionuclide-labeled particles.* Progress in Cardiovascular Diseases, 1977. **20**: p. 55-79.

55. Gregg, D.E., *Effect of coronary perfusion pressure or coronary flow on oxygen usage of the myocardium.* Circulation Research, 1963. **13**: p. 497-500.

56. Weisberg, H., L.N. Katz, and E. Boyd, *Influence of coronary flow upon oxygen consumption and cardiac performance.* Circulation Research, 1963. **13**: p. 522-528.

57. Kahler, R.L., *et al., Effect of alterations of coronary blood flow on the oxygen consumption of the nonworking heart.* Circulation Research, 1963. **13**: p. 501-509.

58. Ross, J.J., *et al., Effect of alteration of coronary blood flow on the oxygen consumption of the working heart.* Circulation Research, 1963. **13**: p. 510-513.

59. Sarnoff, S.J., *et al., Relation between coronary blood flow and myocardial oxygen consumption.* Circulation Research, 1963. **13**: p. 514-521.

60. Daniell, H.B., *Coronary flow alterations on myocardial contractility, oxygen extraction, and oxygen consumption.* American Journal of Physiology, 1973. **225**(5): p. 1020-1025.

61. Homans, D.C., *et al., Subendocardial and subepicardial wall thickening during ischemia in exercising dogs.* Circulation, 1988. **78**(5): p. 1267-1276.

62. Gallagher, K.P., *et al., Effect of exercise on the relationship between myocardial blood flow and systolic wall thickening in dogs with acute coronary stenosis.* Circulation Research, 1983. **52**(6): p. 716-729.

63. Gallagher, K.P., *et al., Regional myocardial perfusion and wall thickening during ischemia in conscious dogs.* American Journal of Physiology, 1984. **247**: p. H727-H738.

64. Gallagher, K.P.*et.al., Significance of regional wall thickening abnormalities relative to transmural myocardial perfusion in anesthetized dogs.* Circulation, 1980. **62**(6): p. 1266-1274.

65. Roan, P.G., *et al., Interrelationships between regional left ventricular function, coronary blood flow, and myocellular necrosis during the initial 24 hours and 1 week after experimental coronary occlusion in awake, unsedated dogs.* Circulation Research, 1981. **49**: p. 31-40.

66. Suga, H., *et al., Critical evaluation of left ventricular systolic pressure volume area as a predictor of oxygen consumption rate.* Japan Journal of Physiology, 1980. **30**: p. 907-919.

67. Suga, H., O. Yamada, and Y. Goto, *Energetics of ventricular contraction as traced in the pressure-volume diagram,.* Federation Proceedings, 1984. **43**(9): p. 2411-2413.

68. Hata, K., et al., *Myocardial oxygen consumption is constant regardless of external mechanical work during relaxation period.* 1991, Circulation: Anaheim. p. 93.

69. Suga, H., *et al., Effect of positive inotropic agents on the relation between oxygen consumption and systolic pressure volume area in canine left ventricle.* Circulation Research, 1983. **53**(September): p. 306-318.

70. Starling, M.R.*et.al., Relation between maximum time-varying elastance pressure-volume areas and myocardial oxygen consumption in dogs.* Circulation, 1991. **83**(1): p. 304-14.

71. Miller, W.P., B.P. Flygenring, and S.H. Nellis, *Effects of load alteration and coronary perfusion pressure on regional end-systolic relations.* Circulation, 1988. **78**(5): p. 1299-1309.

72. Kaseda, S., *et al., End-systolic pressure-volume, pressure-length, and stress-strain relations in canine hearts.* American Journal of Physiology, 1985. **249**: p. H648-H654.

73. Osakada, G., *et al., End-systolic dimension-wall thickness relations during myocardial ischemia in conscious dogs.* The American Journal of Cardiology, 1983. **51**: p. 1750-1758.

74. Tyberg, J.V., *et al., The pressure-length loop; An index of regional cardiac performance in ischemia.* Federation Proceedings, 1973. **32**: p. 343.

75. Tyberg, J.V.*et.al., An analysis of segmental ischemic dysfunction utilizing the pressure-length loop›.* Circulation, 1974. **49**: p. 748-754.

76. Vinten-Johansen, J., *et al., Regional function, blood flow, and oxygen utilization relations in repetitively occluded-reperfused canine myocardium.* American Journal of Physiology, 1991. **261**: p. H538-H547.

77. Safwat, A., *et al., Pressure-length loop area: Its components analyzed during graded myocardial ischemia.* Journal of the American College of Cardiology, 1991. **17**(3): p. 790-796.

78. Sasayama, S.*et.al., Analysis of asynchronus wall motion by regional pressure-length loops in patients with coronary artery disease.* Journal of the American College of Cardiology, 1984. **4**(2): p. 259-267.

79. Hartley, C.J., *et al.*, ed. *High frequency pulsed Doppler measurements of blood flow and myocardial dimensions in conscious animals.* Cardiovascular Instrumentation: Applicability of new technology to biobehavioral research., ed. J.A. Herd, *et al.* 1984, NIH: . 95-106.

80. Pearson, E.S. and H.O. Hartley, *Biometrika Tables for Statisticians.* Third edition ed. Vol. 1. 1966, Cambridge, England: Cambridge University Press.

81. Forrester, J.S., *et al., Pressure-length loop: a new method for simultaneous measurement of segmental and total cardiac function.* Journal of Applied Physiology, 1974. **37**(5): p. 771-775.

82. Braunwald, E. *The determinants of myocardial oxygen consumption.* in *24th International Congress of Physiological Sciences.* 1968. Washington, D.C.: The Physiologist.

83. Weber, K.T. and J.S. Janicki, *Interdependence of cardiac function, coronary flow and oxygen extraction.* American Journal of Physiology, 1978. **235**(6): p. h784-h793.

84. Rooke, A.G., *Low-dose halothane anesthesia does not affect the hemodynamic estimation of myocardial oxygen consumption in dogs.* Anesthesiology, 1990. **72**(4): p. 682-693.

85. Streeter, D.D., *et al., Fiber orientation in the canine left ventricle during diastole and systole.* Circulation Research, 1969. **24**: p. 339-347.

86. Gallagher, K.P.*et.al., Subepicardial segmental function during coronary stenosis and the role of myocardial fiber orientation.* Circulation Research, 1982. **50**(3): p. 352-359.

87. Gallagher, K.P., *et al., Nonuniformity of inner and outer systolic wall thickening in conscious dogs.* American Journal of Physiology, 1985. **249**: p. H241-H248.

88. Vatner, S.F., R.J. McRitchie, and E. Braunwald, *Effects of dobutamine on left ventricular performance, coronary dynamics, and distribution of cardiac function in conscious dogs.* Journal of Clinical Investigation, 1974. **53**: p. 1265-1273.

89. Manders, W.T. and S.F. Vatner, *Effects of sodium pentobarbital anesthesia on left ventricular function and distribution of cardiac output in dogs, with particular reference to the mechanism for tachycardia.* Circulation Research, 1976. **39**(4): p. 512-517.

90. Chatterjee, K., *Effects of dobutamine on coronary hemodynamics and myocardial energetics.*, in *Dobutamine,* K. Chatterjee, Editor. 1989, NCM Publishers, Inc.: New York. p. 49-68.

91. Vatner, S.F. and N.T. Smith, *Effects of halothane on left ventricular function and distribution of regional blood flow in dogs and primates.* Circulation Research, 1974. **34**: p. 155-167.

92. Buckberg, G.D., *et al., Some sources of error in measuring regional blood flow with radioactive microspheres.* Journal of Applied Physiology, 1971. **31**(4): p. 598-604.

93. Canty, J.M., J. Giglia, and D. Kandanth, *Effect of tachycardia on regional function and transmural myocardial perfusion during graded coronary pressure reduction in conscious dogs.* Circulation, 1990. **82**(5): p. 1815-1825.

94. Gallagher, K.P., *et al., Isoproterenol induced myocardial dysfunction in dogs with coronary stenosis.* American Journal of Physiology: Heart Circulation Physiology, 1982. **11**: p. H260-H267.

95. Arts, T. and R.S. Reneman, *Interaction between intramyocardial pressure (IMP) and myocardial circulation.* Journal of Biomechanical Engineering, 1985. **107**: p. 51-56.

96. Baird, R.J., *et al., Intramyocardial pressure: a study of its regional variations and its relationship to intraventricular pressure.* Journal of Thoracic and Cardiovascular Surgery, 1970. **59**: p. 810-823.

97. Brandi, G. and M. McGregor, *Intramyocardial pressure in the left ventricle of the dog.* Cardiovascular Research, 1969. **3**: p. 472-475.

98. Heineman, F.W. and J. Grayson, *Transmural distribution of intramyocardial pressure measured by micropipette technique.* American Journal of Physiology: Heart Circulation Physiology, 1985. **18**: p. H1216-H1223.

99. Pennel, D.J., *et al., Dobutamine -Thallium Myocardial Perfusion Tomography.* Journal of the American College of Cardiology, 1991. **18**: p. 1471-1479.

HARVEY CUSHING / JOHN HAY WHITNEY
MEDICAL LIBRARY

MANUSCRIPT THESES

Unpublished theses submitted for the Master's and Doctor's degrees and deposited in the Medical Library are to be used only with due regard to the rights of the authors. Bibliographical references may be noted, but passages must not be copied without permission of the authors, and without proper credit being given in subsequent written or published work.

This thesis by has been used by the following persons, whose signatures attest their acceptance of the above restrictions.

NAME AND ADDRESS	DATE